



Cooperative adaptive management of the Nile River with climate and socio-economic uncertainties

Received: 16 May 2022

Accepted: 10 November 2022

Published online: 9 January 2023



Mohammed Basheer¹, Victor Nechifor^{2,3}, Alvaro Calzadilla², Solomon Gebrechorkos⁴, David Pritchard⁵, Nathan Forsythe⁵, Jose M. Gonzalez¹, Justin Sheffield⁴, Hayley J. Fowler^{5,6} & Julien J. Harou^{1,7}✉

The uncertainties around the hydrological and socio-economic implications of climate change pose a challenge for Nile River system management, especially with rapidly rising demands for river-system-related services and political tensions between the riparian countries. Cooperative adaptive management of the Nile can help alleviate some of these stressors and tensions. Here we present a planning framework for adaptive management of the Nile infrastructure system, combining climate projections; hydrological, river system and economy-wide simulators; and artificial intelligence multi-objective design and machine learning algorithms. We demonstrate the utility of the framework by designing a cooperative adaptive management policy for the Grand Ethiopian Renaissance Dam that balances the transboundary economic and biophysical interests of Ethiopia, Sudan and Egypt. This shows that if the three countries compromise cooperatively and adaptively in managing the dam, the national-level economic and resilience benefits are substantial, especially under climate projections with the most extreme streamflow changes.

Human activities have increased the atmospheric concentration of GHGs, leading to warming of the Earth's land, atmosphere and ocean^{1–4}. Global initiatives such as the Paris Agreement⁵ and the Sustainable Development Goals⁶ aim to reduce the impacts of climate change by limiting the rise in global temperature and stepping up adaptation efforts. However, the global mean temperature continued to rise over the past two decades, from 0.89 °C in 2001–2010 to 1.09 °C in 2011–2020 above pre-industrial conditions¹. The Nile Basin (Fig. 1) faces the threat of climate change alongside water scarcity, rapidly rising pressures on water resources due to population and economic growth, and a politically complex transboundary water management system. The Nile Basin is located in northeastern Africa, occupies around 10% of the continent's

area and extends over 11 countries. Supplementary Section 1 provides further information on the Nile geography.

Since the beginning of the twentieth century, several large water infrastructure projects have been constructed on the Nile River to reduce the spatial and temporal variabilities of the river flow and to facilitate water supply, flood control and hydropower generation. Most of these infrastructures are in Egypt, Sudan and Ethiopia. Currently, most of the consumptive usage of the Nile streamflow, measured at Aswan, is located in Sudan and Egypt^{7,8}. Over the past two decades, Ethiopia has been increasing its use of the Nile, primarily for hydropower generation. The construction of the Grand Ethiopian Renaissance Dam (GERD) on the Nile near the Ethiopian–Sudanese border (Fig. 1) flared up political

¹Department of Mechanical, Aerospace and Civil Engineering, University of Manchester, Manchester, UK. ²Institute for Sustainable Resources, University College London, London, UK. ³Joint Research Centre, European Commission, Seville, Spain. ⁴School of Geography and Environmental Science, University of Southampton, Southampton, UK. ⁵School of Engineering, Newcastle University, Newcastle upon Tyne, UK. ⁶Tyndall Centre for Climate Change Research, Newcastle University, Newcastle upon Tyne, UK. ⁷Department of Civil, Environmental and Geomatic Engineering, University College London, London, UK. ✉e-mail: julien.harou@manchester.ac.uk

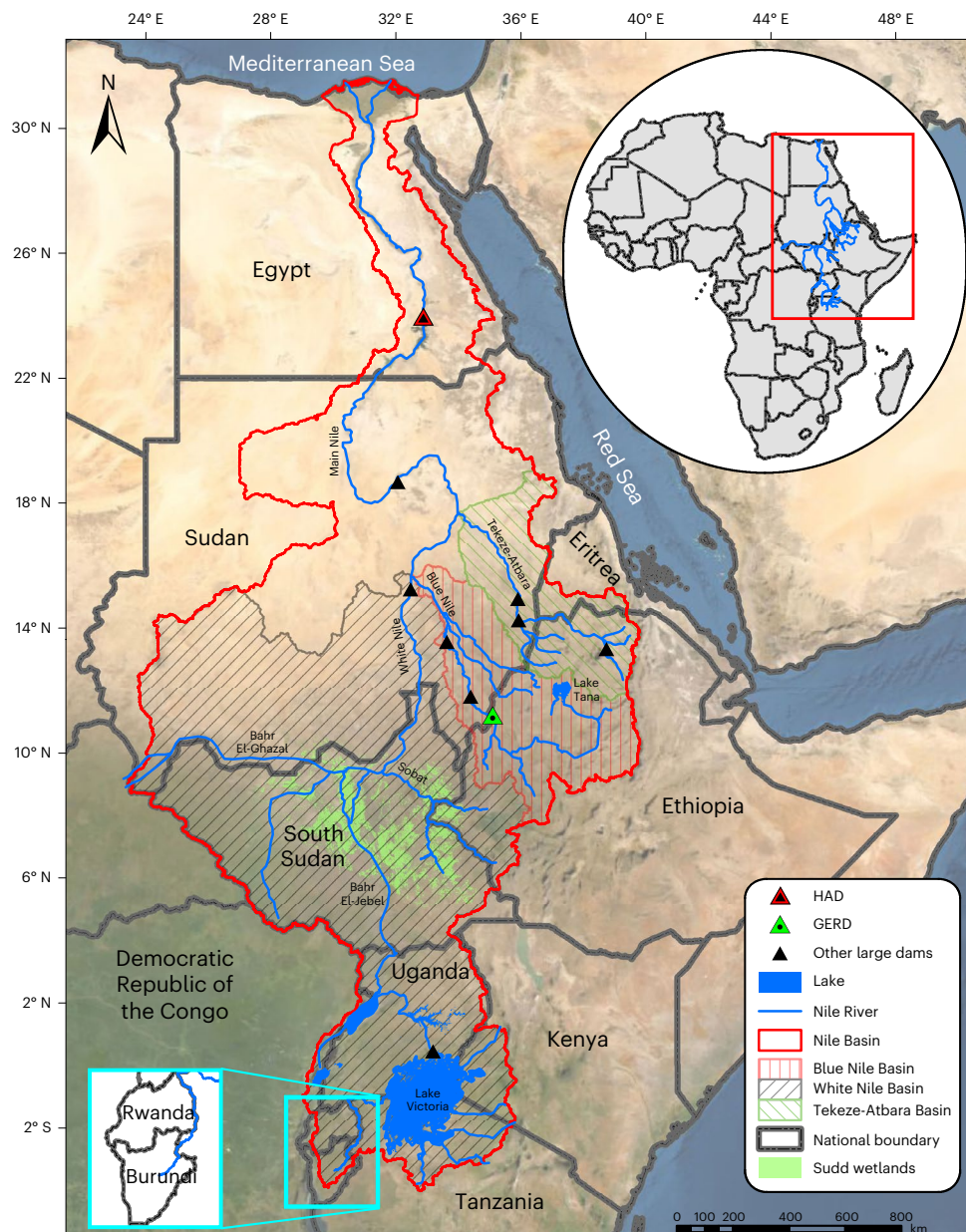


Fig. 1 | The Nile Basin and its major tributaries and dams. The map shows the extents of the basins of the three main tributaries of the Nile: the Blue Nile, the White Nile and the Tekeze-Atbara.

tensions between Ethiopia, Sudan and Egypt on Nile water use^{9–12}. The construction of the GERD started in 2011, and when completed, the dam will have a total storage capacity of 74 billion cubic meters (bcm) and an installed power capacity of 5,150 MW. The total storage capacity of the GERD is equivalent to 1.5 times the historical mean annual river flow at the dam location. The dam is expected to result in a range of opportunities and risks to Sudan and Egypt. Subject to coordination and data sharing, hydropower generation, irrigation water supply reliability and flood control in Sudan could improve because of the dam^{13–16}. Still, the dam will probably produce adverse environmental impacts and losses to recession agriculture in Sudan¹⁷. For Egypt, the GERD is expected to reduce hydropower generation and impose irrigation water deficits if there is no coordination on managing multi-year droughts^{7,12}.

Despite over a decade of negotiations, there is still disagreement and political tension between Ethiopia, Sudan and Egypt on the GERD's initial filling and long-term operation. A milestone in the tripartite

GERD negotiations was a series of meetings held from November 2019 to February 2020, with the United States administration and the World Bank as observers¹⁸. These meetings produced a proposal for the dam's initial filling and long-term operation (hereon referred to as the Washington draft proposal)¹⁹, but the proposal was unacceptable to Ethiopia, which opined that the proposal would limit power generation from the dam and restrain future development²⁰.

Alongside this changing political landscape, the quantity and intensity of rainfall and streamflow in the Nile Basin have changed over the past two decades and are expected to continue to change due to climate change. However, the direction and magnitude of future changes to the Nile climate are uncertain, stemming from different scenarios, modelling and downscaling choices^{21,22}. In the Nile context, these inconsistencies in climate projections diminish the value of using one projection or a multi-model ensemble mean in climate adaptation planning^{22,23}.

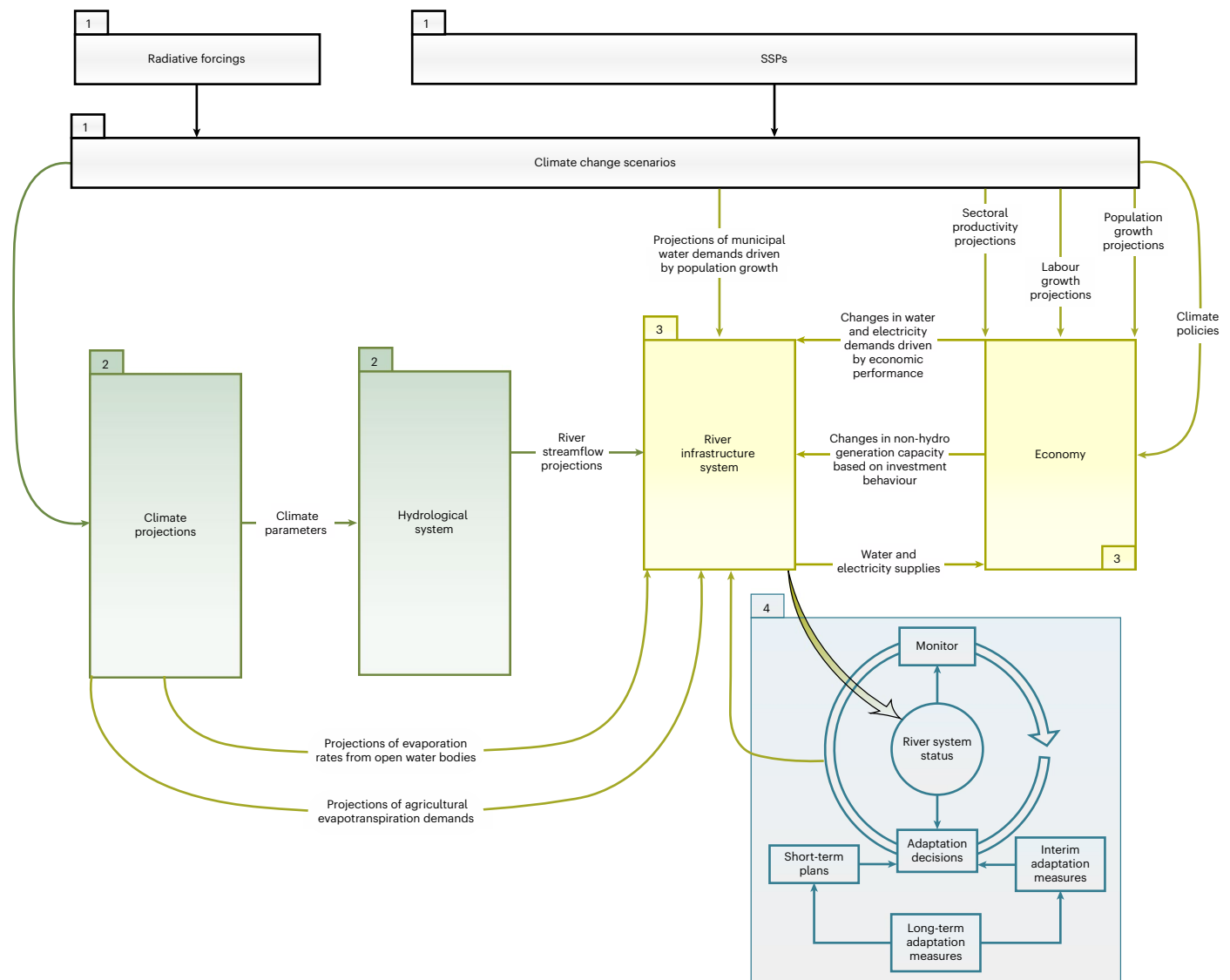


Fig. 2 | Adaptive planning framework for Nile infrastructure management in the face of climate and socio-economic changes. The framework includes four stages numbered from 1 to 4.

The large uncertainties associated with the water resource implications of changes in socio-economic and climate systems motivate adaptive infrastructure development plans^{24–29}. Several approaches have been proposed to enable planning under deep uncertainty^{26,30}; these allow designing robust and flexible plans that maximize resilience and minimize investment costs on the basis of, for example, adaptation tipping points³¹, dynamic adaptive planning³² and dynamic adaptive policy pathways^{24,33}. Several recent studies have applied such adaptive methods to planning water resource systems in various contexts^{25,34–38}. For instance, a reservoir adaptive planning framework has been developed to explicitly consider learning about climate uncertainty over time³⁵, and other studies have optimized the indicators, actions and/or thresholds in the design process of adaptive plans for water resource systems^{33,36,39,40}. However, none of the previous studies considered engineering performance alongside economy-wide performance in the design process of climate adaptation plans for large water infrastructure systems, even though the ultimate goal of building and operating infrastructure is typically to stimulate economic development and generate economy-wide gains.

Here we introduce a planning framework for adaptive management of river infrastructure systems to consider both the socio-economic and hydrological uncertainties of climate change and policy.

The framework uses climate and socio-economic data from the Coupled Model Intercomparison Project 6 (CMIP6)⁴¹ to drive integrated hydrological, economy-wide and river system simulators of the Nile Basin. Our adaptive planning framework uses artificial-intelligence-based algorithms to design efficient adaptive plans for climate change on the basis of thousands of iterations between the algorithms and the integrated simulators. We use the framework to design a cooperative adaptive management policy for the GERD (for 2020–2045) that considers economic and river system interests of Ethiopia, Sudan and Egypt. The results demonstrate that if the GERD is adaptively managed, the economic and resilience benefits to individual countries (especially under extreme climate projections) are substantially larger than with less adaptive responses such as the Washington draft proposal.

Adaptive planning framework for Nile management

In this study, we introduce an adaptive planning framework for managing the Nile infrastructure system in the face of climate and socio-economic changes, including four interconnected stages (Fig. 2): (1) selecting plausible climate change projections, (2) simulating the hydrological implications of the selected projections,

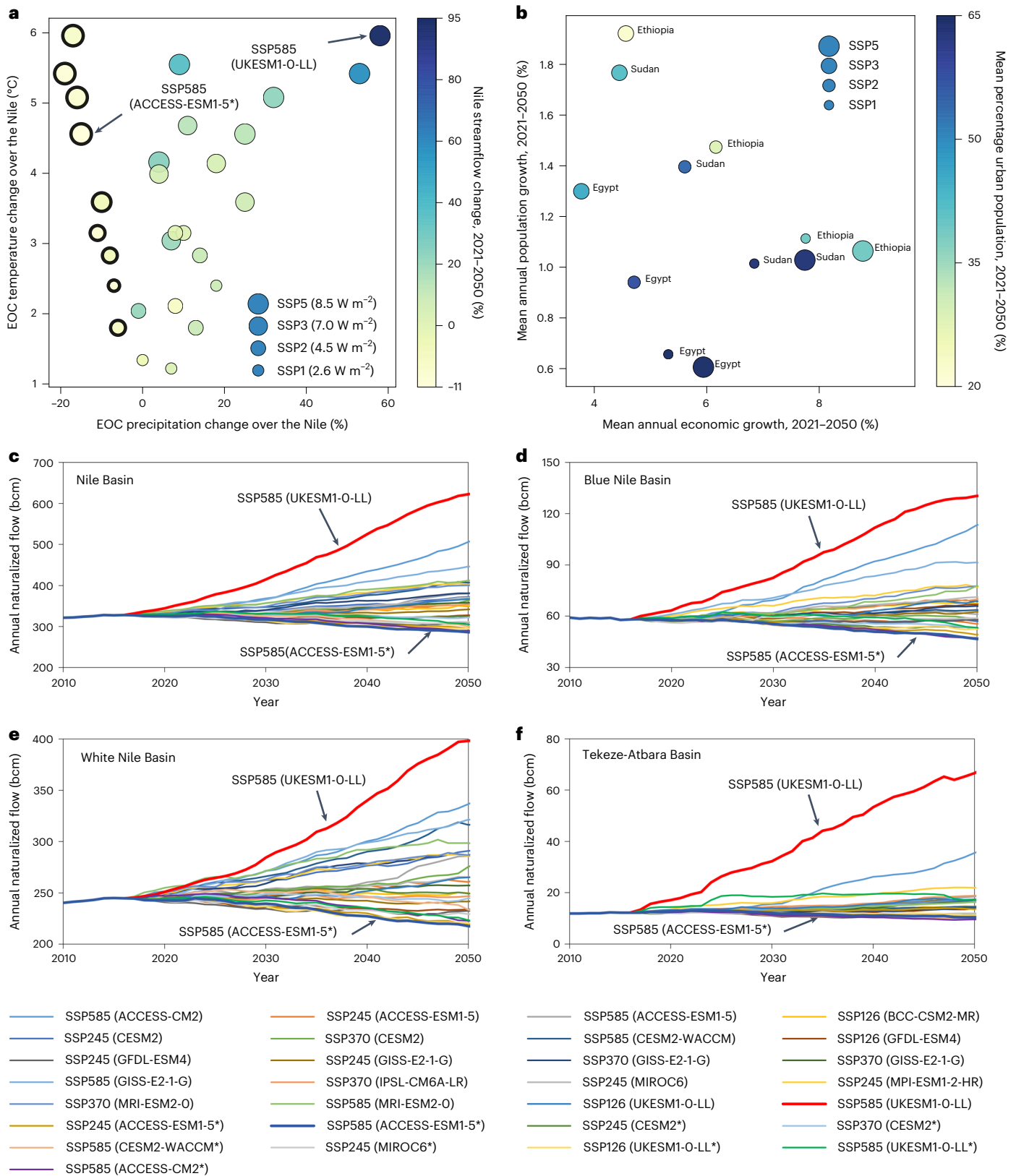


Fig. 3 | Impacts of climate change on the Nile under multiple projections. **a**, Changes in precipitation, naturalized streamflow and temperature. **b**, Socio-economic implications for Ethiopia, Sudan and Egypt. **c–f**, 30-year moving average of the annual naturalized streamflow. The labels in parentheses are the names of the climate models. The change in naturalized streamflow is the percentage change in the mean in 2021–2050 relative to 1981–2016. EOC change in

in precipitation is the percentage change in the mean in 2071–2100 relative to 1981–2010. EOC change in temperature is the absolute change in the mean in 2071–2100 relative to 1981–2010. The climate projections marked with thick black outlines in **a** and with asterisks in **c–f** were synthesized to address the Eastern African Paradox (see Methods for the details).

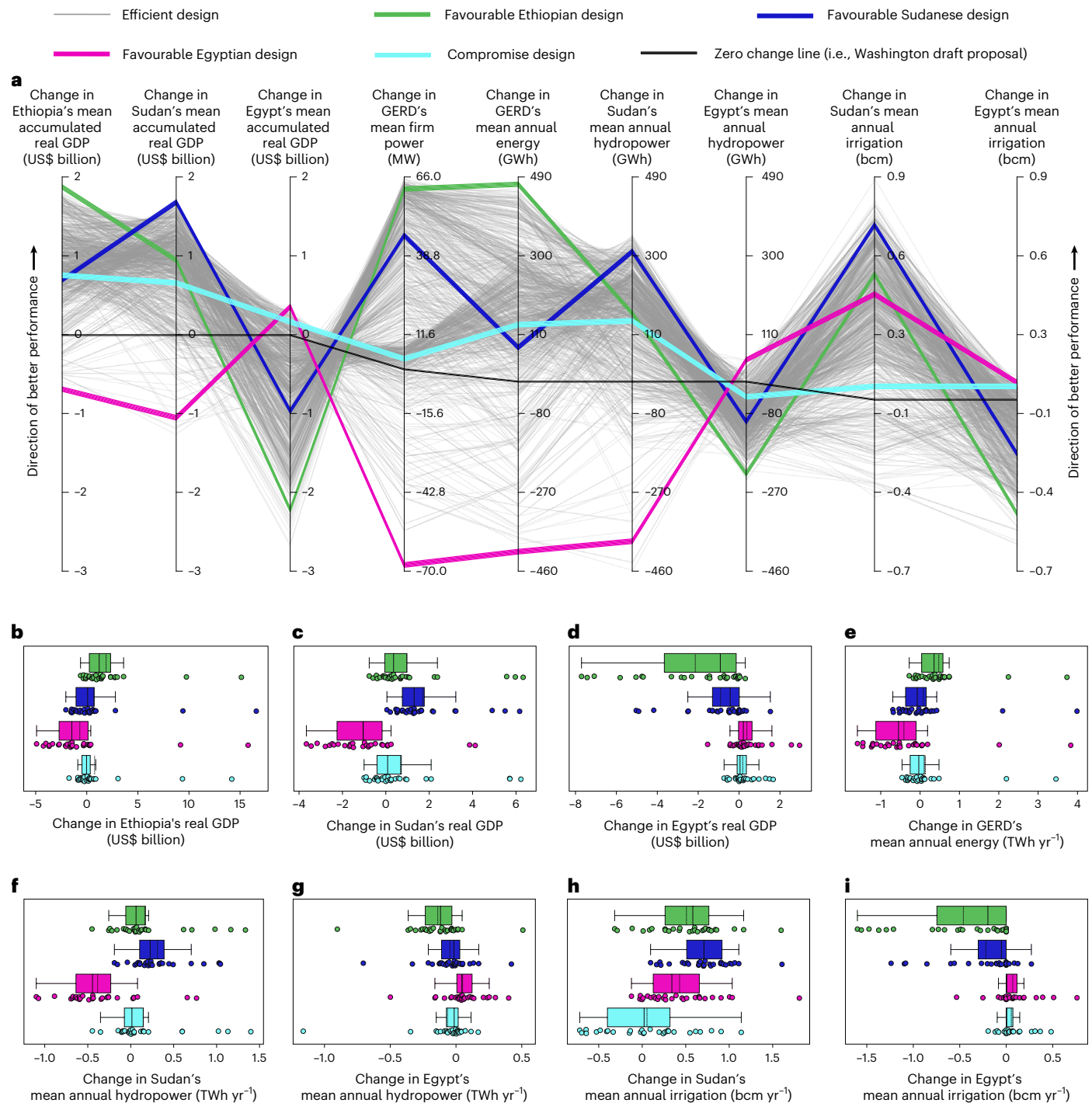


Fig. 4 | Trade-offs and synergies between Ethiopian, Sudanese and Egyptian economy-wide and river system performance objectives. a, Parallel coordinates plot of the performance under efficient designs of an adaptive GERD management policy across 29 climate change projections for 2020–2045. **b–i**, Box plots of some of the metrics shown in **a** for selected designs across the 29 climate change projections. All change values are calculated from a baseline in which the GERD is operated on the basis of the Washington draft proposal.

The box plots in **b–i** correspond to the lines with similar colours in **a**. The ends of the boxes in **b–i** represent the upper and lower quartiles, the solid vertical lines inside the boxes mark the medians, the dashed vertical lines mark the means, the circles show the data points and the whiskers extend to the maximum and minimum values, excluding the outliers. The firm power values are calculated on the basis of a 90% reliability, and the GDP values are discounted at a 3% rate.

(3) simulating the economy-wide and river system infrastructure performance under the selected projections, and (4) designing an adaptive plan for managing river system infrastructure. The four stages are numbered in Fig. 2 from 1 to 4.

In the first stage, 29 transient climate change projections to 2100 were constructed on the basis of bias-corrected CMIP6 Tier 1

simulations⁴¹. Spanning the Shared Socio-economic Pathways (SSPs), 20 general circulation model (GCM) simulations were selected to represent the joint distribution of end-of-century (EOC; 2071–2100) changes in precipitation and temperature over the Nile Basin according to the CMIP6 ensemble. Additionally, nine projections with decreasing precipitation trends were synthesized to counteract the uncertain

precipitation increases often seen in GCMs over East Africa^{42,43} (Methods and Supplementary Table 1). The second stage of the framework is to calibrate and use a distributed hydrological model for the Nile driven by historical climate time series and the 29 climate projections to generate naturalized historical and projected streamflow time series. Furthermore, time series for projected potential evapotranspiration (PET) from irrigation schemes and open water bodies were generated.

Because climate change scenarios have implications for river systems and their economies, the third stage of the framework aims to capture these implications through integrated economy-wide and river system simulators⁷. The river system simulator accounts for all major infrastructure in the Nile Basin in monthly time steps and uses the naturalized streamflow and PET time series generated in the second stage. Furthermore, dynamic-recursive annual computable general equilibrium (CGE) models were developed for Ethiopia, Sudan and Egypt to simulate their economies.

Climate projections may have different global socio-economic development pathways associated with them⁴¹. Accordingly, the CGE models were exogenously driven by national-level projections for labour growth and population growth, total and sectoral productivities, and climate policies that differ with each SSP characterizing the climate projections^{44–46}. Population growth projections under the SSPs were also used to change (that is, increase or decrease) municipal water demands in the river system simulator.

The fourth stage of the framework seeks to design adaptive management policies for the Nile water infrastructure. Climate adaptation planning is achieved using an artificial-intelligence-based approach (multi-objective evolutionary algorithm) to design efficient adaptive management plans. These plans involve adaptation mechanisms based on new information gained about climate change impacts on the river system and riparian countries as the future unravels. The design framework identifies efficient adaptive plans that maximize the riparian countries' economy-wide and river system interests in different ways and reveal trade-offs.

Implications of climate change for the Nile

Under the 29 examined projections, the results show varying impacts of climate change on the naturalized streamflow of the Nile and some socio-economic characteristics of Ethiopia, Sudan and Egypt (Fig. 3). The lower the GHG emissions and EOC forcing levels, the lower the change in precipitation and streamflow (Fig. 3a). The 30-year moving average naturalized streamflow data shown in Fig. 3c–f indicate that the mean Nile streamflow could change by between –13% and +90% by 2050 compared with 2020. The intra-annual variability of the naturalized streamflow of the Nile and its main tributaries is projected to change (Extended Data Fig. 1), with the biggest changes occurring under SSP5 and high EOC temperature projections. The inter-annual streamflow variability shows varying changes depending on different SSPs, forcing levels, GCMs and time horizons, as depicted in Extended Data Fig. 2. The increase in temperature imposed by climate change is projected to increase PET (Extended Data Figs. 3 and 4), which would increase future irrigation water demands and evaporation from open water bodies.

Various SSPs that underpin climate projections have different implications for baseline gross domestic product (GDP) and population growth and urbanization in Ethiopia, Sudan and Egypt over 2021–2050 (Fig. 3b)^{44–46}. The highest economic growth for each of the three countries is projected under SSP5, whereas the lowest economic growth occurs under SSP3.

Cooperative adaptive management policy for the GERD

We use the Nile adaptive management framework to formulate and design an adaptive management policy for the GERD's initial filling and long-term operation for 2020–2045, involving short-term rules and interim and long-term adaptation measures to cope with climate change uncertainties.

The formulation is based on cooperative behaviour whereby the riparian countries consider each other's interests through adaptive measures. The formulation of the GERD adaptive filling and operation policy is described briefly below and detailed in Extended Data Fig. 5.

In the adaptive formulation, water retention during the GERD's initial filling phase is carried out in July and August and follows a stage-based approach (Supplementary Table 2) while maintaining a minimum outflow of 1.28 bcm per month, similar to the Washington draft proposal¹⁹. From March to June, additional interim water releases during the initial filling phase are made if the storage of the High Aswan Dam (HAD) reservoir in Egypt falls below 60 bcm. This would enable quick initial filling of the GERD, as data show consistently high water storage in the HAD reservoir in recent years (2020–2022)⁴⁷.

In the long-term operation phase of the adaptive formulation, GERD water releases aim to generate a regular power target when reservoir storage is above a level termed the power reduction threshold, but this target is reduced as an interim precaution if GERD storage runs lower than a power reduction threshold to allow storage recovery during and following multi-year droughts. To help Egypt during droughts, an interim minimum monthly drought mitigation water release from the GERD is activated if the storage of the HAD reservoir stays below 60 bcm over the past six months for an extended period; this period is termed the drought trigger. This interim drought mitigation measure is activated only if the GERD storage is above a threshold termed the drought outflow storage threshold. The operations of the seasonal storage dams downstream of the GERD follow their historical rules during the GERD's filling phase, whereas their reservoirs are kept as high as possible during the long-term operation phase, similar to assumptions made by previous studies, assuming data sharing between Ethiopia and Sudan^{7,14–16}.

Long-term adaptation measures are applied to the GERD's regular and reduced power targets, the drought trigger of the HAD, and the interim minimum monthly drought mitigation water release. The long-term adaptation measures are triggered on a five-year interval, involving increasing or decreasing these four GERD management variables on the basis of the change in the mean annual inflow to the dam over the past five years in relation to the historical mean annual inflow over 1980–2019. For instance, if the mean annual inflow to the GERD increased over the past five years compared with the historical mean, the four above-mentioned GERD operation variables are increased proportionally, and vice versa.

The artificial-intelligence-based search component of the framework was used to design the adaptive GERD management policy described above. The search algorithm optimizes seven variables; these variables and their upper and lower bounds are reported in Supplementary Table 3. The variables are designed to maximize nine objectives of Ethiopia, Sudan and Egypt over 2020–2045 across the 29 climate change projections: the accumulated GDP values of each country (three objectives); the GERD's 90% firm power (one objective); the annual hydro-energy generation of the GERD, Sudan and Egypt (three objectives); and the annual irrigation water use in Sudan and Egypt (two objectives).

Economic and river system benefits of adaptive GERD management

The results reveal differences between the aggregated economy-wide and river system performance objectives over 2020–2045 under 1,032 efficient GERD adaptive management options and the performance under the Washington draft proposal, as shown in the parallel coordinates plot⁴⁸ depicted in Fig. 4a. The reader is referred to Supplementary Section 2, Supplementary Table 2 and Extended Data Fig. 6 for the implementation details of the Washington draft proposal. Four efficient adaptive GERD policy designs are highlighted in Fig. 4a (the green, blue, purple and cyan lines): a favourable design for each of Ethiopia, Sudan and Egypt that results in the highest national accumulated GDP benefits, and an example compromise design that results in

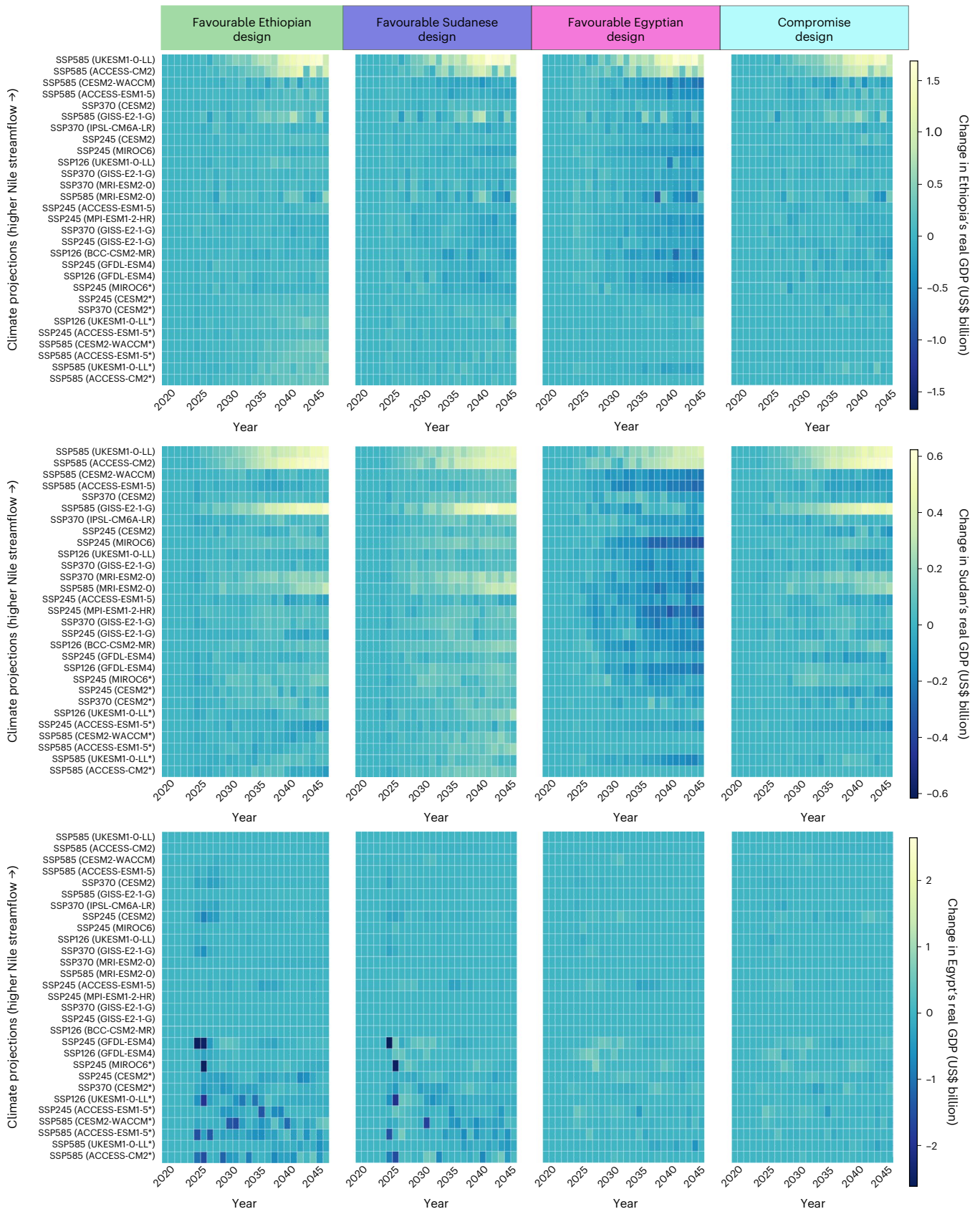


Fig. 5 | Heatmap matrix of changes in the Ethiopian, Sudanese and Egyptian real GDP for four adaptive policy designs. The GDP changes are for the four designs of the GERD’s adaptive policy highlighted in Fig. 4a compared with a baseline in which the GERD is operated on the basis of the Washington draft proposal. Each row of the matrix shows GDP changes for one of the three

countries, whereas the matrix columns correspond to different designs of the adaptive management policy for the GERD. The labels in parentheses are the names of the climate models. The changes in real GDP are discounted at a 3% rate. The climate projections marked with asterisks were synthesized to address the Eastern African Paradox.

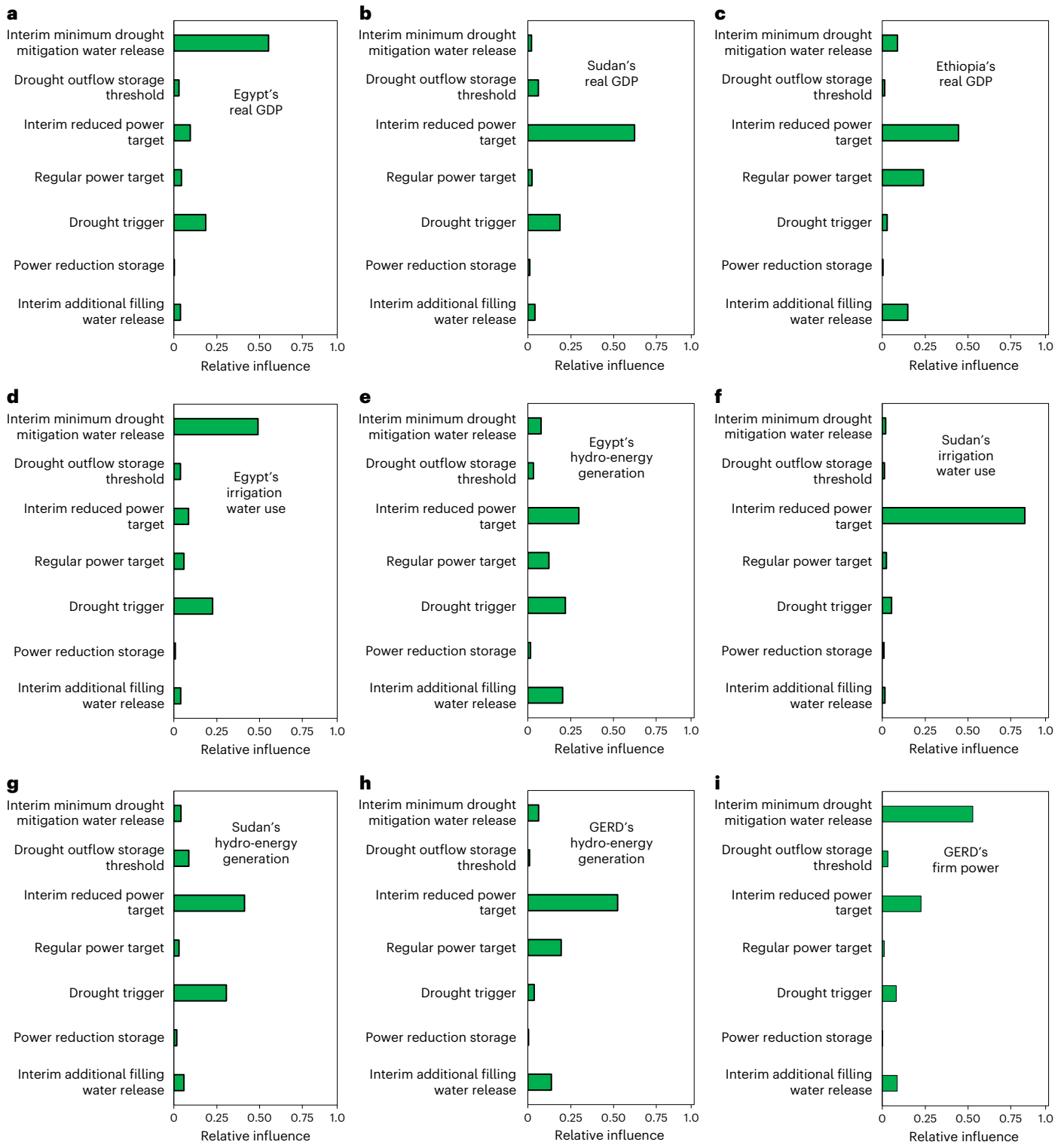


Fig. 6 | Rankings of the variables of the adaptive management policy for the GERD based on their relative influence on nine economic and river system performance metrics. a–i, The relative influence values are based on machine learning and can range from zero to one, with zero indicating that the variable

does not influence the performance metric, whereas one indicates that the variable is the sole influencer of the performance metric. For each performance metric, the sum of the relative influence values for all parameters is one.

at least 40% of the highest national accumulated GDP benefits for each of the three countries. The specifications of the four highlighted GERD policy designs are in Supplementary Table 4 and Supplementary Fig. 2. The results show that the magnitudes of the economy-wide costs and benefits to Ethiopia, Sudan and Egypt vary due to the different

economies and the spatial and temporal characteristics of the river system in each country. There is a trade-off between the three countries in achieving the highest possible GDP performance. Compared with the Washington draft proposal, the compromise design results in economy-wide benefits to the three countries.

The results reveal varying costs and benefits across climate projections (Fig. 4b–i). For instance, in the most favourable design for each country taken individually, the discounted GDP over 2020–2045 could increase by up to US\$15.8, US\$6.3 and US\$3.0 billion for Ethiopia, Sudan and Egypt, respectively, compared with the Washington draft proposal. However, these country-centric designs lead to GDP losses for at least one of the other two countries. In contrast, the mean GDP changes are positive for the three countries under the compromise design.

The temporal evolution of GDP changes under different climate projections and GERD policy designs (Fig. 5) shows that adaptive GERD management benefits Ethiopia and Sudan the most under climate projections with the highest streamflow. The favourable Egyptian design benefits Egypt during multi-year droughts in climate projections with low streamflow, but it reduces the overall Sudanese and Ethiopian benefits (Fig. 5). The compromise system design results in balanced performance across the three countries.

The seven optimized variables of the GERD adaptive policy show varying influence on the Ethiopian, Sudanese and Egyptian performance objectives (Fig. 6). The Egyptian GDP is influenced the most by the interim minimum drought mitigation water releases (Fig. 6a), as most of Egypt's benefits and costs materialize during droughts through irrigation. In contrast, the most influential parameter for the Sudanese and Ethiopian GDPs is the GERD's reduced power target (Fig. 6b,c). For Sudan, decreases in GERD water releases due to power reduction influence irrigation (Fig. 6f) and hydropower (Fig. 6g) because of the absence of multi-year storage dams to buffer this variability.

Discussion

Because the Nile River is crucial to its population's economic development and well-being, adaptation strategies are needed to cope with the deep uncertainties associated with future climate change^{26,49}. An approach that can identify efficient options for transboundary adaptation and demonstrate their economy-wide and river system benefits and trade-offs could provide a platform for discussions on Nile adaptation strategies. The adaptive planning framework introduced in this paper can design adaptive policies for large infrastructures to cope with climate change uncertainties. Using a meta-heuristic artificial-intelligence-based algorithm for the search process provides twofold benefits. First, it enables finding multi-dimensionally efficient (Pareto-optimal) solutions for complex and highly nonlinear interlinked river and economic systems. Second, it optimizes on the basis of linked but independent simulation models developed by different disciplines. Although the proposed framework can capture direct and induced impacts of climate change and infrastructure management policies on river and economy systems, it should be complemented with approaches to assess other impacts on groundwater, river ecology and riparian populations^{7,50}.

The analysis of the GERD's initial filling and long-term operation shows that adaptively managing the dam to maximize the national benefits of any of the three countries would be costly for at least one of the other two countries. We show that a compromise adaptive management approach could produce balanced benefits for the three countries. These results demonstrate the opportunity cost of not implementing collaborative adaptive solutions, especially under extreme climate change projections. It is high time to integrate climate change adaptation into the decade-long negotiations between Ethiopia, Sudan and Egypt over the GERD and the broader Nile management discussion between the 11 riparian countries.

Although the adaptive formulation examined in this study includes some controlling features (for example, the 60-bcm HAD drought threshold and the five-year adaptation period) that constrain basin-wide water management, it represents an incremental step towards adaptive cooperation. Our goal is to show that any step towards adaptive cooperation results in benefits. Such an incremental approach can help build trust between riparian countries and make an eventual unconstrained basin-wide adaptive management easier to

achieve, aiming to maximize basin-wide benefits, adopt benefit-sharing and build on the comparative advantages of each riparian country.

Practical use of the proposed framework in Nile negotiations requires riparian countries to negotiate an adaptive formulation and define the ranges within which decisions can be optimized. The philosophy behind the adaptive formulation should be guided by a long-term vision to counter future climate and socio-economic uncertainties. The efficient cooperative adaptive designs emanating from the agreed formulation should then be negotiated to find a compromise solution that balances national-level and basin-wide performance.

Online content

Any methods, additional references, Nature Portfolio reporting summaries, source data, extended data, supplementary information, acknowledgements, peer review information; details of author contributions and competing interests; and statements of data and code availability are available at <https://doi.org/10.1038/s41558-022-01556-6>.

References

1. IPCC *Climate Change 2021: The Physical Science Basis* (eds Masson-Delmotte, V. et al.) (Cambridge Univ. Press, 2021).
2. Wigley, T. M. L. & Raper, S. C. B. Natural variability of the climate system and detection of the greenhouse effect. *Nature* **344**, 324–327 (1990).
3. Crowley, J. T. Causes of climate change over the past 1000 years. *Science* **289**, 270–277 (2000).
4. Wang, W. C., Yung, Y. L., Laci, A. A., Mo, T. A. & Hansen, J. E. Greenhouse effects due to man-made perturbations of trace gases. *Science* **194**, 685–690 (1976).
5. *Paris Agreement* (United Nations Framework Convention on Climate Change, 2015).
6. Rio+20 United Nations Conference on Sustainable Development *The Future We Want: Outcome Document of the United Nations Conference on Sustainable Development* (United Nations, 2012).
7. Basheer, M. et al. Collaborative management of the Grand Ethiopian Renaissance Dam increases economic benefits and resilience. *Nat. Commun.* **12**, 5622 (2021).
8. *Agreement between the Republic of the Sudan and the United Arab Republic for the Full Utilization of the Nile Waters* (International Water Law Project, 1959); http://internationalwaterlaw.org/documents/regionaldocs/uar_sudan.html
9. Cascão, A. E. & Nicol, A. GERD: new norms of cooperation in the Nile Basin? *Water Int.* **41**, 550–573 (2016).
10. Salman, S. The Grand Ethiopian Renaissance Dam: the road to the declaration of principles and the Khartoum document. *Water Int.* **41**, 512–527 (2016).
11. Tawfik, R. The Grand Ethiopian Renaissance Dam: a benefit-sharing project in the Eastern Nile? *Water Int.* **41**, 574–592 (2016).
12. Wheeler, K. G., Jeuland, M., Hall, J. W., Zagana, E. & Whittington, D. Understanding and managing new risks on the Nile with the Grand Ethiopian Renaissance Dam. *Nat. Commun.* <https://doi.org/10.1038/s41467-020-19089-x> (2020).
13. Wheeler, K. et al. Exploring cooperative transboundary river management strategies for the Eastern Nile Basin. *Water Resour. Res.* <https://doi.org/10.1029/2017WR022149> (2018).
14. Wheeler, K. G. et al. Cooperative filling approaches for the Grand Ethiopian Renaissance Dam. *Water Int.* **41**, 611–634 (2016).
15. Basheer, M. et al. Quantifying and evaluating the impacts of cooperation in transboundary river basins on the water–energy–food nexus: the Blue Nile Basin. *Sci. Total Environ.* **630**, 1309–1323 (2018).
16. Basheer, M. Cooperative operation of the Grand Ethiopian Renaissance Dam reduces Nile riverine floods. *River Res. Appl.* **47**, 805–814 (2021).

17. Elagib, N. A. & Basheer, M. Would Africa's largest hydropower dam have profound environmental impacts? *Environ. Sci. Pollut. Res.* **28**, 8936–8944 (2021).
18. *Joint Statement of Egypt, Ethiopia, Sudan, the United States and the World Bank* (United States Department of the Treasury, 2020); <https://home.treasury.gov/news/press-releases/sm891>
19. Edrees, M. Letter dated 11 June 2021 from the Permanent Representative of Egypt to the United Nations addressed to the Secretary-General (United Nations, 2021); <https://digitallibrary.un.org/record/3931750?ln=en>
20. Amde, T. A. Letter dated 14 May 2020 from the Permanent Representative of Ethiopia to the United Nations addressed to the President of the Security Council (United Nations, 2020); <https://digitallibrary.un.org/record/3862715?ln=en>
21. Taye, M. T., Willems, P. & Block, P. Implications of climate change on hydrological extremes in the Blue Nile Basin: a review. *J. Hydrol. Reg. Stud.* **4**, 280–293 (2015).
22. Di Baldassarre, G. et al. Future hydrology and climate in the River Nile Basin: a review. *Hydrol. Sci. J.* **56**, 199–211 (2011).
23. Bhattacharjee, P. S. & Zaitchik, B. F. Perspectives on CMIP5 model performance in the Nile River headwaters regions. *Int. J. Climatol.* **35**, 4262–4275 (2015).
24. Haasnoot, M., Kwakkel, J. H., Walker, W. E. & ter Maat, J. Dynamic adaptive policy pathways: a method for crafting robust decisions for a deeply uncertain world. *Glob. Environ. Change* **23**, 485–498 (2013).
25. Hui, R., Herman, J., Lund, J. & Madani, K. Adaptive water infrastructure planning for nonstationary hydrology. *Adv. Water Resour.* **118**, 83–94 (2018).
26. Marchau, V. A. W. J., Walker, W. E., Bloemen, P. J. T. M. & Popper, S. W. (eds) *Decision Making under Deep Uncertainty: From Theory to Practice* (Springer, 2019).
27. Smith, M. et al. *Adaptation's Thirst: Accelerating the Convergence of Water and Climate Action* (Global Commission on Adaptation, 2019).
28. Hallegatte, S. Strategies to adapt to an uncertain climate change. *Glob. Environ. Change* **19**, 240–247 (2009).
29. Reed, P. M. et al. Multisector dynamics: advancing the science of complex adaptive human–Earth systems. *Earth's Future* **10**, e2021EF002621 (2022).
30. Walker, W. E., Haasnoot, M. & Kwakkel, J. H. Adapt or perish: a review of planning approaches for adaptation under deep uncertainty. *Sustainability* **5**, 955–979 (2013).
31. Kwadijk, J. C. J. et al. Using adaptation tipping points to prepare for climate change and sea level rise: a case study in the Netherlands. *WIREs Clim. Change* **1**, 729–740 (2010).
32. Kwakkel, J. H., Walker, W. E. & Marchau, V. Adaptive airport strategic planning. *Eur. J. Transp. Infrastruct. Res.* **10**, 249–273 (2010).
33. Kwakkel, J. H., Haasnoot, M. & Walker, W. E. Developing dynamic adaptive policy pathways: a computer-assisted approach for developing adaptive strategies for a deeply uncertain world. *Climatic Change* **132**, 373–386 (2015).
34. Zeff, H. B., Herman, J. D., Reed, P. M. & Characklis, G. W. Cooperative drought adaptation: integrating infrastructure development, conservation, and water transfers into adaptive policy pathways. *Water Resour. Res.* <https://doi.org/10.1002/2016WR018771> (2016).
35. Fletcher, S., Lickley, M. & Strzepek, K. Learning about climate change uncertainty enables flexible water infrastructure planning. *Nat. Commun.* **10**, 1782 (2019).
36. Cohen, J. S. & Herman, J. D. Dynamic adaptation of water resources systems under uncertainty by learning policy structure and indicators. *Water Resour. Res.* **57**, e2021WR030433 (2021).
37. Ricalde, I. et al. Assessing tradeoffs in the design of climate change adaptation strategies for water utilities in Chile. *J. Environ. Manage.* **302**, 114035 (2022).
38. Pachos, K., Huskova, I., Matrosov, E., Erfani, T. & Harou, J. J. Trade-off informed adaptive and robust real options water resources planning. *Adv. Water Resour.* **161**, 104117 (2022).
39. Gold, D. F., Reed, P. M., Gorelick, D. E. & Characklis, G. W. Power and pathways: exploring robustness, cooperative stability, and power relationships in regional infrastructure investment and water supply management portfolio pathways. *Earth's Future* **10**, e2021EF002472 (2022).
40. Beh, E. H. Y., Maier, H. & Dandy, G. C. Adaptive, multiobjective optimal sequencing approach for urban water supply augmentation under deep uncertainty. *Water Resour. Res.* <https://doi.org/10.1002/2014WR016254> (2015).
41. O'Neill, B. C. et al. The Scenario Model Intercomparison Project (ScenarioMIP) for CMIP6. *Geosci. Model Dev.* **9**, 3461–3482 (2016).
42. Wainwright, C. M. et al. 'Eastern African Paradox' rainfall decline due to shorter not less intense Long Rains. *NPJ Clim. Atmos. Sci.* **2**, 34 (2019).
43. Rowell, D. P., Booth, B. B. B., Nicholson, S. E. & Good, P. Reconciling past and future rainfall trends over East Africa. *J. Clim.* **28**, 9768–9788 (2015).
44. Riahi, K. et al. The Shared Socioeconomic Pathways and their energy, land use, and greenhouse gas emissions implications: an overview. *Glob. Environ. Change* **42**, 153–168 (2017).
45. KC, S. & Lutz, W. The human core of the Shared Socioeconomic Pathways: population scenarios by age, sex and level of education for all countries to 2100. *Glob. Environ. Change* **42**, 181–192 (2017).
46. Crespo Cuaresma, J. Income projections for climate change research: a framework based on human capital dynamics. *Glob. Environ. Change* **42**, 226–236 (2017).
47. *Water Level* (Copernicus Global Land Service, 2022); <https://land.copernicus.eu/global/products/wl>
48. Inselberg, A. in *Trends in Interactive Visualization: State-of-the-Art Survey* (eds Liere, R. et al.) 49–78 (Springer, 2009).
49. Goulden, M., Conway, D. & Persechino, A. Adaptation to climate change in international river basins in Africa: a review. *Hydrol. Sci. J.* **54**, 805–828 (2009).
50. Dasgupta, P. *The Economics of Biodiversity: The Dasgupta Review* (HM Treasury, 2021).

Publisher's note Springer Nature remains neutral with regard to jurisdictional claims in published maps and institutional affiliations.

Open Access This article is licensed under a Creative Commons Attribution 4.0 International License, which permits use, sharing, adaptation, distribution and reproduction in any medium or format, as long as you give appropriate credit to the original author(s) and the source, provide a link to the Creative Commons license, and indicate if changes were made. The images or other third party material in this article are included in the article's Creative Commons license, unless indicated otherwise in a credit line to the material. If material is not included in the article's Creative Commons license and your intended use is not permitted by statutory regulation or exceeds the permitted use, you will need to obtain permission directly from the copyright holder. To view a copy of this license, visit <http://creativecommons.org/licenses/by/4.0/>.

© The Author(s) 2023

Methods

Here we introduce an adaptive planning framework for the Nile Basin that combines climate change projections; integrated hydrological, economy-wide and river system simulators; and multi-objective evolutionary and machine learning algorithms. Below is a description of the components and data of the framework.

Climate projections

Twenty climate projections were selected from CMIP6 Tier 1 GCMs on the basis of uniform sampling to cover the full range of available SSPs, radiative forcing and the joint distribution of EOC change in precipitation and temperature over the Nile Basin. Processing, down-scaling and bias correction of the GCM simulations were driven by the requirement for transient (2017–2100) three-hourly forcing data across seven climate variables that govern the surface mass and energy balances in the hydrological model (described in the next section). The seven variables are precipitation, temperature, incoming shortwave radiation, incoming longwave radiation, humidity, wind speed and surface pressure. Given the large spatial domain, the low availability of subdaily model output for all of the relevant variables in CMIP6 and challenges of multivariate bias correction⁵¹, we derived bias-corrected transient projections by (1) resampling the 0.25° historical baseline climate dataset to match the (detrended) relative variability of the selected GCM projections and then (2) applying perturbation factors to reintroduce the change signal extracted from the GCMs following a quantile delta mapping approach⁵².

In more detail, we first detrended the basin-average monthly future precipitation series for 2017–2100 in each GCM run on a month-wise basis using smoothed 37-year moving averages. Second, we ranked the detrended future series month-wise and matched the ranks to their equivalents in the historical baseline precipitation dataset of 1981–2016, allowing us to construct synthetic climate series for 2017–2100 at the three-hour temporal resolution of the historical climate datasets by inserting the relevant month of data from the historical dataset at the right place in the future series. The synthesized series thus have the same overall sequencing of relative intra-annual (seasonal), interannual and multi-annual variability as the original GCM projections in rank terms, while preserving the statistical properties (including spatial, temporal and intervariable consistency^{53,54}) and resolution of the historical baseline dataset (that is, without GCM bias). The historical baseline climate datasets used are the Multi-Source Weighted-Ensemble Precipitation (MSWEP)⁵⁵ for precipitation and the Princeton Global Forcing (PGF)⁵⁶ for the other climate variables. The 0.1° MSWEP data were regridded to the 0.25° PGF grid before the climate series was synthesized.

For each of the 20 climate projections, we then reintroduced the climate change signal to the synthesized 2017–2100 climate series, producing bias-corrected and perturbed projections. The transient climate change signal was reintroduced on a month-wise basis using a 37-year moving window of quantile-based perturbations⁵². Smoothing was applied to the perturbation factors via a moving average to avoid any jumps between successive windows. We note that this method does not adjust the frequency of wet periods/days within a month, and it is not designed to focus on projected changes in precipitation extremes, given the study's focus on water resources management on a monthly scale rather than flood frequency.

Several previous studies have highlighted how the wetting trend in climate projections for eastern Africa stands in contrast to the observed decline in precipitation from the 1980s to the late 2000s⁴². This contradiction, known as the Eastern African Paradox, represents a challenge for climate adaptation planning^{42,43}. While the literature shows a growing understanding of how this issue is linked with regional circulation dynamics and their representation in models^{57,58}, there is not yet a consensus on how the projections might be constrained. Yet, if the projections are taken at face value, there is a risk that adaptation

measures are designed for a highly uncertain wetter climate that might not materialize, with potentially severe socio-economic consequences.

To address this issue, we synthesized nine additional scenarios based on 9 of the 20 initial projections by removing the overall wetting tendency in the CMIP6 ensemble for the East Africa region. The magnitude of the tendency was estimated by quantifying the mean increase in EOC mean precipitation for a unit increase in mean temperature according to the full GCM ensemble, given their strong relationship in this context. The relationship was then used to adjust individual GCM precipitation trends downwards, allowing us to select the nine projections representing the most pessimistic scenarios in terms of precipitation decreases, which enables stress-testing adaptation policies across a wide range of plausible futures (Fig. 3a). Supplementary Table 1 lists the 29 projections and their main features. Daily PET was calculated for the 29 projections using the FAO56 Penman–Monteith method⁵⁹.

Hydrological simulator

To generate time series of historical and projected naturalized streamflow for the Nile Basin, we used and calibrated the Variable Infiltration Capacity (VIC version 5) land surface model⁶⁰ and the Routing Application for Parallel Computation of Discharge (RAPID)⁶¹. The VIC and RAPID models were originally developed in a previous study to reconstruct vector-based global naturalized streamflow⁶². The hydrological model has a spatial resolution of 0.25° and a three-hourly temporal resolution. The historical streamflow time series was driven by MSWEP⁵⁵ and temperature, incoming shortwave radiation, incoming longwave radiation, humidity, wind speed and surface pressure data from the PGF⁵⁶. The 29 projected streamflow time series were driven by similar climate variables obtained from the climate projections described in the previous section. The VIC and RAPID models were calibrated against a historical naturalized streamflow dataset of the Nile previously developed for the Eastern Nile Technical Regional Office⁶³. The hydrological model was calibrated using baseflow parameters, depth of soil layers, variable infiltration curve and maximum soil moisture. Supplementary Table 5 shows the ranges of the values of the calibration parameters for all grid cells in the hydrological model. The RAPID model routes streamflow using the Muskingum method⁶⁴ and requires a river network to determine Muskingum parameters (that is, the gradient coefficient and the weighting factor). The river network was obtained from the Hydrological data and maps on the basis of Shuttle Elevation Derivatives at multiple Scales (HydroSHEDS)⁶⁵. The hydrological model was calibrated over the period 1982–1992 and validated over 1993–2002 at four locations where naturalized flow data are available. Supplementary Table 6 shows the performance of the hydrological model in the calibration and validation periods, and Supplementary Table 7 summarizes the model performance ranking criteria adopted. As elaborated in the next section, the combined hydrological and river system simulator was calibrated at additional locations.

River system simulator

To simulate the performance of the Nile River system infrastructure under climate change and various adaptive management options, we developed a monthly river system model for the basin using Python Water Resources (Pywr)⁶⁶. A river system model is a network representation of the supplies, demands and infrastructures of water resources in a river system⁶⁷. Pywr is an open-source Python library that simulates resource networks. It enables representing water resources system infrastructure (for example, dams, lakes, aquifer-based water supply and water abstraction locations) in a network structure driven by water supplies (for example, hydrological inflows) and demands (for example, irrigation, municipal and industrial water demands and hydropower) and system operating rules. Pywr uses a linear programming approach to simulate water allocations at each time step (monthly in this study) subject to constraints imposed by system operation rules. Supplementary Fig. 3 shows a schematic of the Nile River system model

and its elements, and Supplementary Table 8 shows the main features of the dams included in the model. The model uses the naturalized stream-flow time series of the Nile generated using the hydrological model described in the previous section. Data for dams, lakes, reservoirs, and irrigation and municipal water demands were collected from different sources, including the Nile Basin Initiative and previous studies^{44,15,68–71}.

In simulating future scenarios, the water demands of irrigation schemes and the net evaporation rates of lakes, reservoirs and swamps were modified (increased or decreased) on the basis of the annual change ratio of PET at their locations relative to the historical annual mean. Extended Data Figs. 3 and 4 show the projected annual change in PET relative to the historical mean at some selected dams and irrigation schemes in the Nile River system. Future municipal water demands were calculated by applying the population growth rates projected under different climate change scenarios (that is, SSPs). The population growth projections under different SSPs were obtained from the International Institute for Applied Systems Analysis (IIASA) database^{44,45}. Supplementary Section 3 describes the initial water demand assumptions for Ethiopia, Sudan and Egypt.

The Nile River system simulator was calibrated and validated at ten locations over 1995–2010 using historical river flow observations and reservoir and lake water levels. This calibration period was chosen on the basis of the availability of common and continuous historical observed data for the ten selected locations. Supplementary Fig. 4 and Supplementary Table 9 show the performance of the Nile River system model over the calibration and validation periods. Supplementary Table 10 reports the calibration parameters and their values, and Supplementary Table 7 reports the performance ranking criteria. Total non-hydro (for example, thermal) generation for each country was represented as a super generator used to fill the gap between hydropower generation and national electricity demand subject to generation capacity. The non-hydro generation capacity and national electricity demands are updated annually on the basis of an iterative process between the river system and the economy-wide simulators, as described in a later section.

Economy-wide simulator

The standard open-source CGE model of the International Food Policy Research Institute⁷² was modified and used to develop economy-wide models for Ethiopia, Sudan and Egypt. The production and consumption specifications in the CGE models are shown in Supplementary Figs. 5 and 6. The CGE models were set up to run dynamically over multi-year periods (that is, dynamic-recursive) following endogenous investment behaviour, exogenous total and sectoral factor productivities, labour growth, and energy use efficiency trends.

The CGE models of Ethiopia, Sudan and Egypt include five agent types: households, the government, enterprises, industries (or economic activities) and the rest of the world. Households are disaggregated into rural and urban groups. Ethiopia's, Sudan's and Egypt's CGE models include 12, 15 and 14 economic activities, respectively. Economic activities use the following factors of production: labour, general capital, land, hydropower capital, non-hydro capital, renewables capital, water supply capital, oil capital and gas capital. Labour and general capital are assumed mobile between sectors, whereas the other factors are sector-specific. All capital types, except water supply and hydropower capitals, grow or shrink over time on the basis of investment behaviour according to relative rates of return. Water supply and hydropower capitals were not included in the year-to-year investment behaviour, as expansion in these infrastructures typically requires abrupt investment in the Nile context.

We assume that commodity prices on the international market are exogenous, following the small open-economy assumption⁷³. The government is assumed to spend a fixed share of total absorption. Saving propensities are fixed, and the exchange rate is variable. The CGE models were calibrated to social accounting matrices for 2011 obtained

from the International Food Policy Research Institute^{74–76}. We then used the GTAP-Power 10 database for the year 2014⁷⁷ to disaggregate the electricity sectors of the social accounting matrices. Five dynamic baselines were calibrated for the CGE models of Ethiopia, Sudan and Egypt, with each baseline corresponding to an SSP. The baseline total factor productivity values were set up such that the baseline models follow projected economic growth (obtained from the IIASA database) for each SSP scenario⁴⁶. After that, the total factor productivity values were fixed and applied exogenously. Labour growth (16–64 age group)⁴⁵, urbanization⁷⁸ and population growth⁴⁵ projections for each of the three countries were obtained from the IIASA database and applied exogenously to the CGE models. Also, projections for national-level sectoral productivity under each SSP were obtained from the Centre d'Études Prospectives et d'Informations Internationales⁷⁹ and applied exogenously to the CGE models. Sectoral future energy use efficiency values were calibrated such that the baseline simulated country-level carbon dioxide emissions in the baselines follow the growth pattern of the regional emission values of the Middle East and North Africa projected by IIASA for each SSP⁸⁰. Carbon dioxide emissions were calculated in the CGE models by applying emission factors (tons of carbon per terajoule) to the use of petroleum, gas and coal commodities in the economies.

Because the CGE models were calibrated on the basis of 2011 social accounting matrices, they were first run dynamically over 2011–2019 to bring the economies to the first year of the GERD's initial filling before scenarios for 2020–2045 were assessed. The temporal evolution of the values of some of the key driving parameters and baseline outputs of the CGE models are shown in Supplementary Fig. 7.

Economy and river system coupling

The river system infrastructure and economy-wide simulators were connected using a generic co-evolutionary framework developed in a previous study⁷. The framework enables linking river system simulation models (with daily or monthly time steps) with dynamic-recursive annual CGE models. At each annual time step, the coupling framework performs an iterative bidirectional communication between the river system and the CGE simulators to ensure coherence in the annual national-scale irrigation water supply and demand, municipal water supply and demand, hydropower generation, non-hydro generation and capacity, and electricity demand. In each iteration over an annual time step, the river system model quantifies and spatially aggregates national-scale irrigation and municipal water supplies and hydro and non-hydro generation on the basis of the river system's spatial and temporal constraints, infrastructure, and external drivers. This information is then passed to the CGE models as an external shock on the basis of which changes to the economy's municipal and irrigation water demands, electricity demand, and non-hydro capacity are determined and passed back to the river system model for the next iteration. Iterations over each annual time step can be terminated by a maximum number of iterations and/or a convergence error. In this work, we specified a maximum of three iterations between the river system and the economy-wide simulators for each annual time step and a convergence error of US\$5 million measured using the Ethiopian real GDP. The coupling framework is implemented using the open-source Python Network Simulation framework⁸¹. The reader is referred to Basheer et al.⁷ for further details about the co-evolutionary coupling framework used in this study.

Multi-method artificial-intelligence-based design and learning

In the Nile adaptive planning framework, an artificial-intelligence-based multi-objective evolutionary algorithm (MOEA) provides the ability to identify efficient adaptive management policies for river system infrastructure. Supplementary Fig. 8 shows the interaction between the integrated economy-wide and river system simulators and the MOEA.

The MOEA generates a design (that is, a set of decision variable values) for the adaptive management policy (the yellow box in Supplementary Fig. 8), which is then passed to the integrated economy-wide and river system simulators. The integrated model performs a dynamic multi-year multi-scenario simulation considering socio-economic and hydrological uncertainties related to climate change, resulting in aggregated performance metrics (over time and projections) that are indicated as objectives. The adaptive management design and objective values are then stored before proceeding to the next iteration, in which the MOEA suggests new adaptive management designs. The iteration between the MOEA and the integrated simulators continues until a stopping criterion is met. In this study, we use a maximum number of iterations as a criterion to terminate iteration between the integrated simulators and the MOEA. A maximum of 6,000 iterations (or function evaluations) was specified as a stopping criterion for the search process of adaptive GERD management. With every iteration, the MOEA learns from the previous generations of iterations and attempts to suggest an adaptive infrastructure management design that improves performance as measured by the objectives. Once the stopping criterion is met, a non-dominated sorting process is performed to filter efficient adaptive management policies. We used the open-source Non-dominated Sorting Genetic Algorithm III (NSGA-III)⁸² as an MOEA for adaptive design. Platypus, an open-source Python-based framework for evolutionary computing⁸³, was used, which supports NSGA-III.

The multi-objective search was performed for the adaptive management formulation for the GERD with five random seeds. Each seed represents a unique starting condition for the search algorithm. The use of multiple seeds allows checking that the search has converged to a global, approximately optimal set of solutions. A total of 30,000 iterations were therefore performed during the search process (that is, five seeds multiplied by 6,000 iterations). Optimization convergence was tested by calculating the evolution of the hypervolume⁸⁴ for each random seed (Supplementary Fig. 9).

We used machine learning as a post-processing step for understanding the relative influence of adaptive policy variables on economy-wide and river system performance, on the basis of a similar approach to a previous study on economy systems⁸⁵. The values of the adaptive policy variables and the objectives generated during the search iterations between the MOEA and the integrated simulators are used to train a machine learning model for each objective. Accordingly, the features of each machine learning model are the variables of the adaptive policy, and the target is each of the objectives. The Random Forest Regression Machine Learning Algorithm⁸⁶ was used. After the machine learning models were trained, feature importance was calculated, which, for each model, represents the relative influence of features on an objective. The Random Forest Regression Algorithm was used through the open-source Scikit-learn Python library⁸⁷.

For the GERD application, 80% of the data on the objectives and decision variables were used to train 100 tree predictors for each machine learning model, and 20% of the data were used to test performance. Maximum tree depth values from 1 to 30 were tested for each machine learning model. The lowest tree depth that provided a good prediction ability while avoiding overfitting or underfitting the data was selected for each machine learning model. Supplementary Fig. 10 shows the performance of the machine learning models with the training and testing data with different maximum tree depths and the chosen maximum tree depth values.

Implementation of the GERD adaptive management formulation

The GERD adaptive management formulation optimized in this study includes nine objectives and seven decision variables. The objectives maximize the following aggregate metrics over 2020–2045:

1. The mean (over projections) accumulated (discounted over time) Ethiopian real GDP
2. The mean (over projections) accumulated (discounted over time) Sudanese real GDP
3. The mean (over projections) accumulated (discounted over time) Egyptian real GDP
4. The mean (over projections) 90% firm (over time) power generation of the GERD
5. The mean (over projections and time) annual energy generation of the GERD
6. The mean (over projections and time) annual energy from hydropower in Sudan
7. The mean (over projections and time) annual energy from hydropower in Egypt
8. The mean (over projections and time) annual irrigation water supply in Sudan
9. The mean (over projections and time) annual irrigation water supply in Egypt

The seven decision variables are (see Extended Data Fig. 5 for the details):

1. Interim additional filling water release
2. Power reduction storage
3. Regular power target
4. Interim reduced power target
5. Drought trigger
6. Drought outflow storage threshold
7. Interim minimum drought mitigation water release

The upper and lower bounds of the seven decision variables are reported in Supplementary Table 3. Long-term adaptation measures are applied to the regular power target, the interim reduced power target, the drought trigger and the interim minimum drought mitigation water release. The adaptation measures involve increasing or decreasing these four GERD operation variables dynamically on a five-year interval on the basis of how the mean annual inflow to the GERD over the past five years changed in relation to the historical mean annual inflow over 1980–2019.

Reporting summary

Further information on research design is available in the Nature Portfolio Reporting Summary linked to this article.

Data availability

The economy-related input data supporting this study's findings are available at Zenodo⁸⁸: <https://doi.org/10.5281/zenodo.5914757>. The Nile River system model and its data are not publicly available due to state restrictions and contain information that could compromise research participant privacy/consent. The Nile model data can be made available upon presentation of the necessary permissions from the relevant authorities that own the data. The CMIP6 climate projections data can be accessed from <https://esgf-node.llnl.gov/search/cmip6/>. The baseline population, labour, urbanization and economic growth data of Ethiopia, Sudan and Egypt associated with the SSPs can be accessed from the IIASA database at <https://tntcat.iiasa.ac.at/SspDb/dsd?Action=htmlpage&page=10>. The sectoral productivity projections of Ethiopia, Sudan and Egypt were produced on the basis of data from the Centre d'Études Prospectives et d'Informations Internationales at http://www.cepii.fr/cepii/en/bdd_modele/bdd.asp. The MSWEP data are available from <http://www.gloh2o.org/mswep/>. The PGF data are available from <https://rda.ucar.edu/datasets/ds314.0/>. The river network data used with RAPID are freely accessible from <https://www.hydrosheds.org/>. The World Bank data referred to in the manuscript are freely accessible from <https://data.worldbank.org/>.

Code availability

The Pywr simulation model (version 1.9.1) is open-source and freely available at <https://github.com/pywr/pywr>, and building Pywr models can be facilitated by www.waterstrategy.org. The standard CGE model of the International Food Policy Research Institute is open-source and freely accessible through the following link: <https://www.ifpri.org/publication/standard-computable-general-equilibrium-cge-model-gams-0>. The VIC (version 5) model is freely accessible through the following link: <https://vic.readthedocs.io/en/master/>. RAPID (version 1.8.0) is freely accessible through the following link: <http://rapid-hub.org/index.html>. The Python Network Simulation framework (version 0.1.5) is open-source and freely available in the following repository: <https://github.com/UMWRG/pynsim>. The multi-objective NSGA-III, the MOEA used in the multi-objective search, is open-source and freely available through Platypus (version 1.0.4) in the following repository: <https://github.com/Project-Platypus/Platypus>. The Random Forest Regression Algorithm is open-source and freely available through Scikit-learn (version 0.24.2) at <https://github.com/scikit-learn/scikit-learn>.

References

51. François, B., Vrac, M., Cannon, A. J., Robin, Y. & Allard, D. Multivariate bias corrections of climate simulations: which benefits for which losses? *Earth Syst. Dyn.* **11**, 537–562 (2020).
52. Cannon, A. J., Sobie, S. R. & Murdock, T. Q. Bias correction of GCM precipitation by quantile mapping: how well do methods preserve changes in quantiles and extremes? *J. Clim.* **28**, 6938–6959 (2015).
53. Mehrotra, R. & Sharma, A. A resampling approach for correcting systematic spatiotemporal biases for multiple variables in a changing climate. *Water Resour. Res.* **55**, 754–770 (2019).
54. Vrac, M. & Friederichs, P. Multivariate-intervariable, spatial, and temporal-bias correction. *J. Clim.* **28**, 218–237 (2015).
55. Beck, H. E. et al. MSWEP v2 global 3-hourly 0.1° precipitation: methodology and quantitative assessment. *Bull. Am. Meteorol. Soc.* **100**, 473–500 (2019).
56. Sheffield, J., Goteti, G. & Wood, E. F. Development of a 50-year high-resolution global dataset of meteorological forcings for land surface modeling. *J. Clim.* **19**, 3088–3111 (2006).
57. Walker, D. P., Marsham, J. H., Birch, C. E., Scaife, A. A. & Finney, D. L. Common mechanism for interannual and decadal variability in the East African Long Rains. *Geophys. Res. Lett.* **47**, e2020GL089182 (2020).
58. King, J. A. & Washington, R. Future changes in the Indian Ocean Walker Circulation and links to Kenyan rainfall. *J. Geophys. Res. Atmos.* **126**, e2021JD034585 (2021).
59. Allen, R. G., Pereira, L. S., Raes, D. & Smith, M. *FAO Irrigation and Drainage Paper: Crop Evapotranspiration* (FAO, 1998).
60. Liang, X., Lettenmaier, D. P., Wood, E. F. & Burges, S. J. A simple hydrologically based model of land surface water and energy fluxes for general circulation models. *J. Geophys. Res.* **99**, 14415–14428 (1994).
61. David, C. H. et al. River network routing on the NHDPlus dataset. *J. Hydrometeorol.* **12**, 913–934 (2011).
62. Lin, P. et al. Global reconstruction of naturalized river flows at 2.94 million reaches. *Water Resour. Res.* **55**, 6499–6516 (2019).
63. *Development of the Eastern Nile Water Simulation Model* (Deltares, 2013).
64. Gill, M. A. Flood routing by the Muskingum method. *J. Hydrol.* **36**, 353–363 (1978).
65. Lehner, B. & Grill, G. Global river hydrography and network routing: baseline data and new approaches to study the world's large river systems. *Hydrol. Process.* **27**, 2171–2186 (2013).
66. Tomlinson, J. E., Arnott, J. H. & Harou, J. J. A water resource simulator in Python. *Environ. Model. Softw.* **126**, 104635 (2020).
67. Wurbs, R. A. *Generalized Models of River System Development and Management* (IntechOpen, 2011).
68. Basheer, M., Sulieman, R. & Ribbe, L. Exploring management approaches for water and energy in the data-scarce Tekeze-Atbara Basin under hydrologic uncertainty. *Int. J. Water Resour. Dev.* **37**, 182–207 (2021).
69. Basheer, M. & Elagib, N. A. Sensitivity of water–energy nexus to dam operation: a water–energy productivity concept. *Sci. Total Environ.* **616–617**, 918–926 (2018).
70. Basheer, M. et al. Filling Africa's largest hydropower dam should consider engineering realities. *One Earth* **3**, 277–281 (2020).
71. Jeuland, M., Wu, X. & Whittington, D. Infrastructure development and the economics of cooperation in the Eastern Nile. *Water Int.* <https://doi.org/10.1080/O2508060.2017.1278577> (2017).
72. Lofgren, H., Lee, R., Robinson, S., Thomas, M. & El-Said, M. A *Standard Computable General Equilibrium (CGE) Model in GAMS* (International Food Policy Research Institute, 2002).
73. Armington, P. S. A theory of demand for products distinguished by place of production. *Staff Pap.* **16**, 159–178 (1969).
74. Siddig, K., Elagra, S., Grethe, H. & Mubarak, A. *A Post-separation Social Accounting Matrix for the Sudan* (International Food Policy Research Institute, 2018); <https://doi.org/10.2499/1024320695>
75. Al-Riffai, P. et al. *A Disaggregated Social Accounting Matrix: 2010/11 for Policy Analysis in Egypt* (International Food Policy Research Institute, 2016); <http://ebrary.ifpri.org/cdm/ref/collection/p15738coll2/id/130736>
76. Ahmed, H. A., Tebekew, T. & Thurlow, J. *2010/11 Social Accounting Matrix for Ethiopia: A Nexus Project SAM* (International Food Policy Research Institute, 2017); <http://ebrary.ifpri.org/utills/getfile/collection/p15738coll2/id/131505/filename/131720.pdf>
77. Chepeliev, M. Gtap-Power data base: version 10. *J. Glob. Econ. Anal.* **5**, 110–137 (2020).
78. Jiang, L. & O'Neill, B. C. Global urbanization projections for the Shared Socioeconomic Pathways. *Glob. Environ. Change* **42**, 193–199 (2017).
79. Fouré, J., Bénassy-Quéré, A. & Fontagné, L. Modelling the world economy at the 2050 horizon. *Econ. Transit. Inst. Change* **21**, 617–654 (2013).
80. Gidden, M. J. et al. Global emissions pathways under different socioeconomic scenarios for use in CMIP6: a dataset of harmonized emissions trajectories through the end of the century. *Geosci. Model Dev.* **12**, 1443–1475 (2019).
81. Knox, S., Meier, P., Yoon, J. & Harou, J. J. A Python framework for multi-agent simulation of networked resource systems. *Environ. Model. Softw.* **103**, 16–28 (2018).
82. Deb, K. & Jain, H. An evolutionary many-objective optimization algorithm using reference-point-based nondominated sorting approach, part I: solving problems with box constraints. *IEEE Trans. Evol. Comput.* **18**, 577–601 (2014).
83. Hadka, D. Platypus. *GitHub* <https://github.com/Project-Platypus/Platypus> (2016).
84. Zitzler, E., Thiele, L., Laumanns, M., Fonseca, C. M. & Da Fonseca, V. G. Performance assessment of multiobjective optimizers: an analysis and review. *IEEE Trans. Evol. Comput.* **7**, 117–132 (2003).
85. Basheer, M. et al. Balancing national economic policy outcomes for sustainable development. *Nat. Commun.* **13**, 5041 (2022).
86. Breiman, L. Random Forests. *Mach. Learn.* **45**, 5–32 (2001).
87. Pedregosa, F. et al. Scikit-learn: machine learning in Python. *J. Mach. Learn. Res.* **12**, 2825–2830 (2011).
88. Basheer, M., Nechifor, V., Calzadilla, A., Harou, J. J., Data related to a study on adaptive management of Nile infrastructure. *Zenodo* <https://doi.org/10.5281/zenodo.5914757> (2022).

Acknowledgements

M.B.'s doctoral degree is funded by the Faculty of Science and Engineering of the University of Manchester. This work was supported by the UK Research and Innovation Economic and Social Research Council (grant no. ES/PO11373/1) as part of the Global Challenges Research Fund through the 'Future Design and Assessment of water-energy-food-environment Mega Systems' (FutureDAMS) research project to J.J.H., V.N., A.C., S.G., D.P., N.F., J.S. and H.J.F. We thank GAMS Software GmbH for providing licences for mathematical solvers compatible with parallel processing used for economy-wide simulation on supercomputers. We acknowledge the use of the Computational Shared Facility and High-Performance Computing of the University of Manchester. The views expressed in this paper are the sole responsibility of the authors and do not necessarily reflect those of their institutions.

Author contributions

M.B. wrote the original manuscript. M.B. performed the visualization of the results. All authors reviewed and edited the manuscript. M.B. developed the adaptive framework linking various data and model components. M.B. developed and calibrated the Nile River system model. V.N., M.B. and A.C. developed and calibrated the economy-wide models of Ethiopia, Sudan and Egypt. S.G., M.B. and J.S. developed and calibrated the hydrological model of the Nile Basin. D.P., N.F. and H.J.F. processed and bias-corrected the climate

projections. M.B. performed the simulation and optimization work. M.B., J.J.H., V.N. and A.C. conceptualized the study. M.B. formulated the adaptive policy of the Nile. J.J.H. acquired the funding. All authors contributed to the validation and interpretation of the results.

Competing interests

The authors declare no competing interests.

Additional information

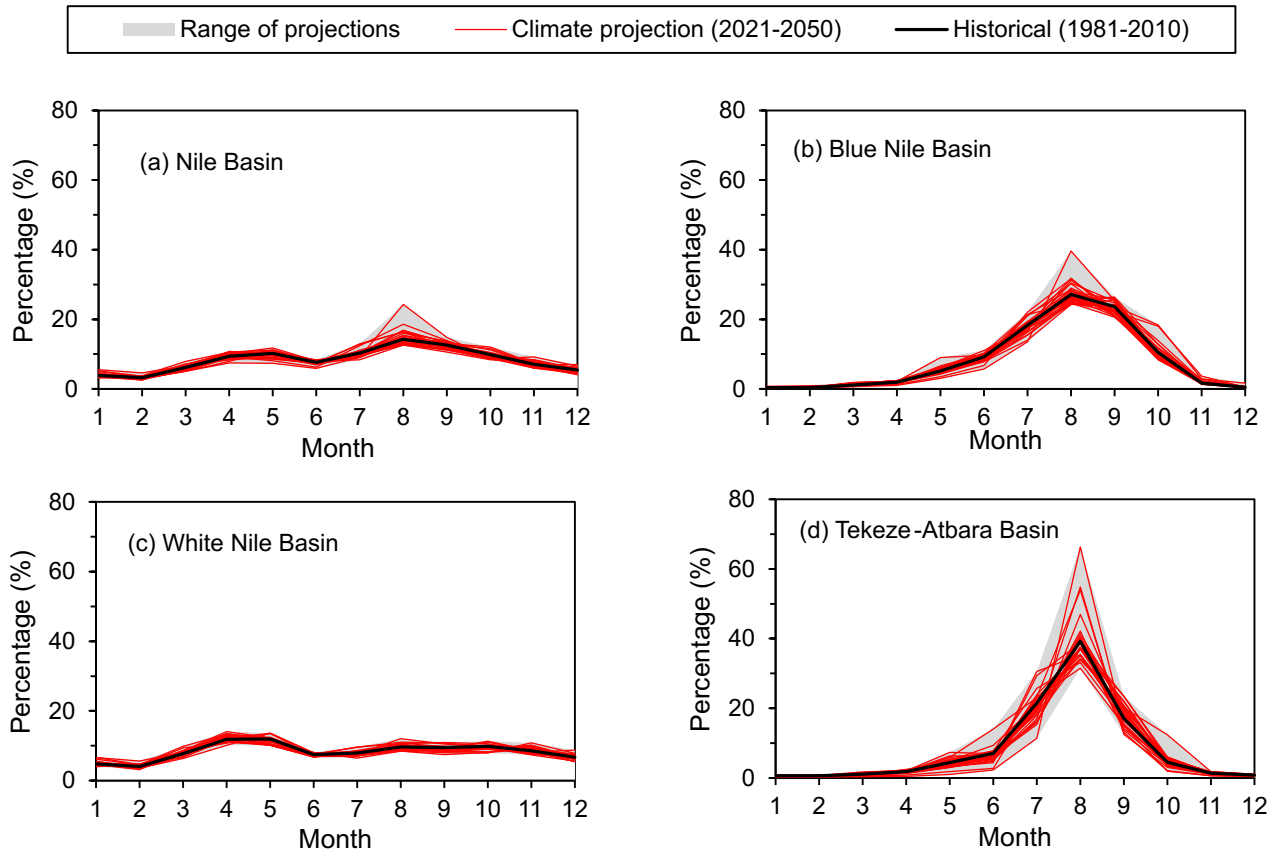
Extended data is available for this paper at <https://doi.org/10.1038/s41558-022-01556-6>.

Supplementary information The online version contains supplementary material available at <https://doi.org/10.1038/s41558-022-01556-6>.

Correspondence and requests for materials should be addressed to Julien J. Harou.

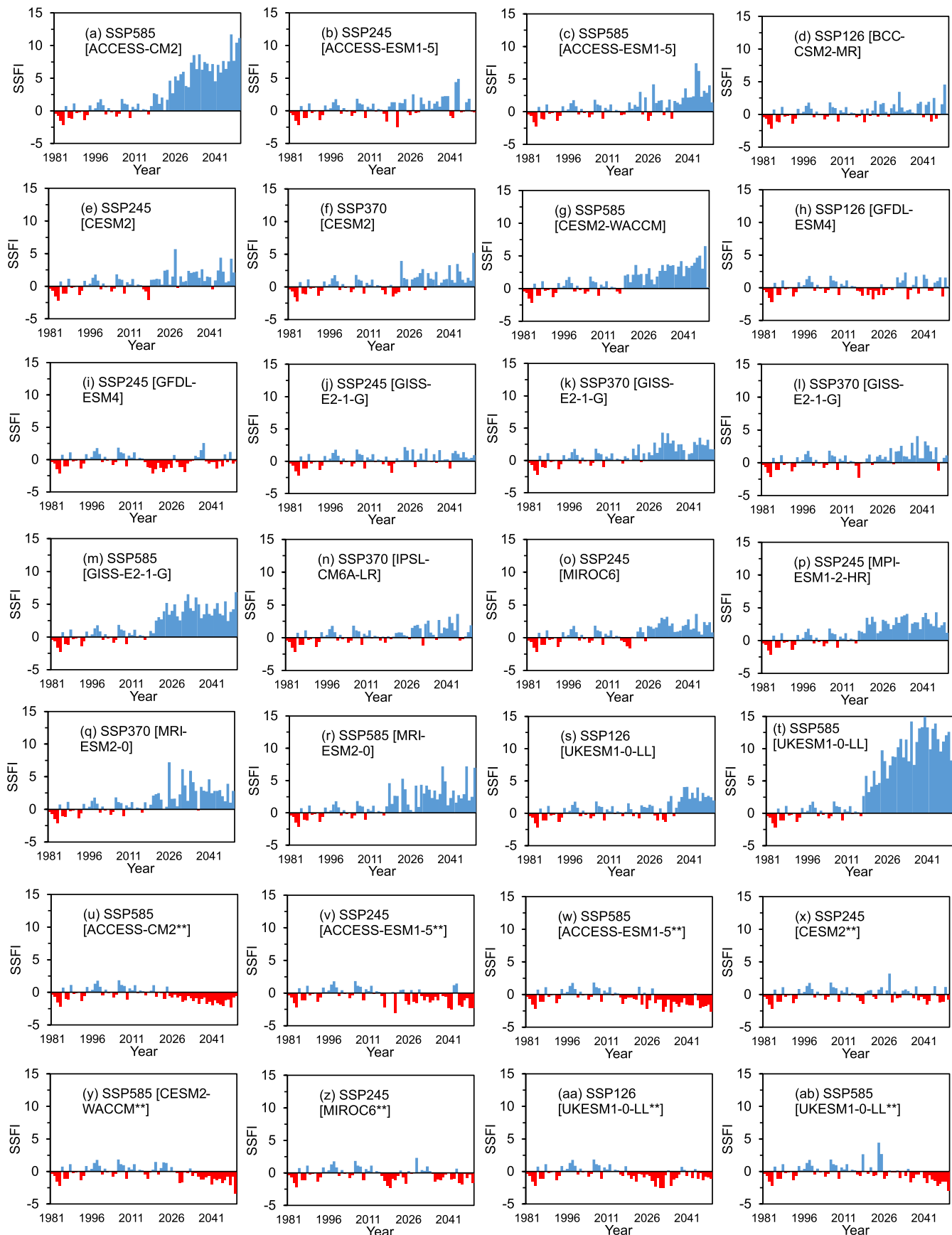
Peer review information *Nature Climate Change* thanks the anonymous reviewers for their contribution to the peer review of this work.

Reprints and permissions information is available at www.nature.com/reprints.



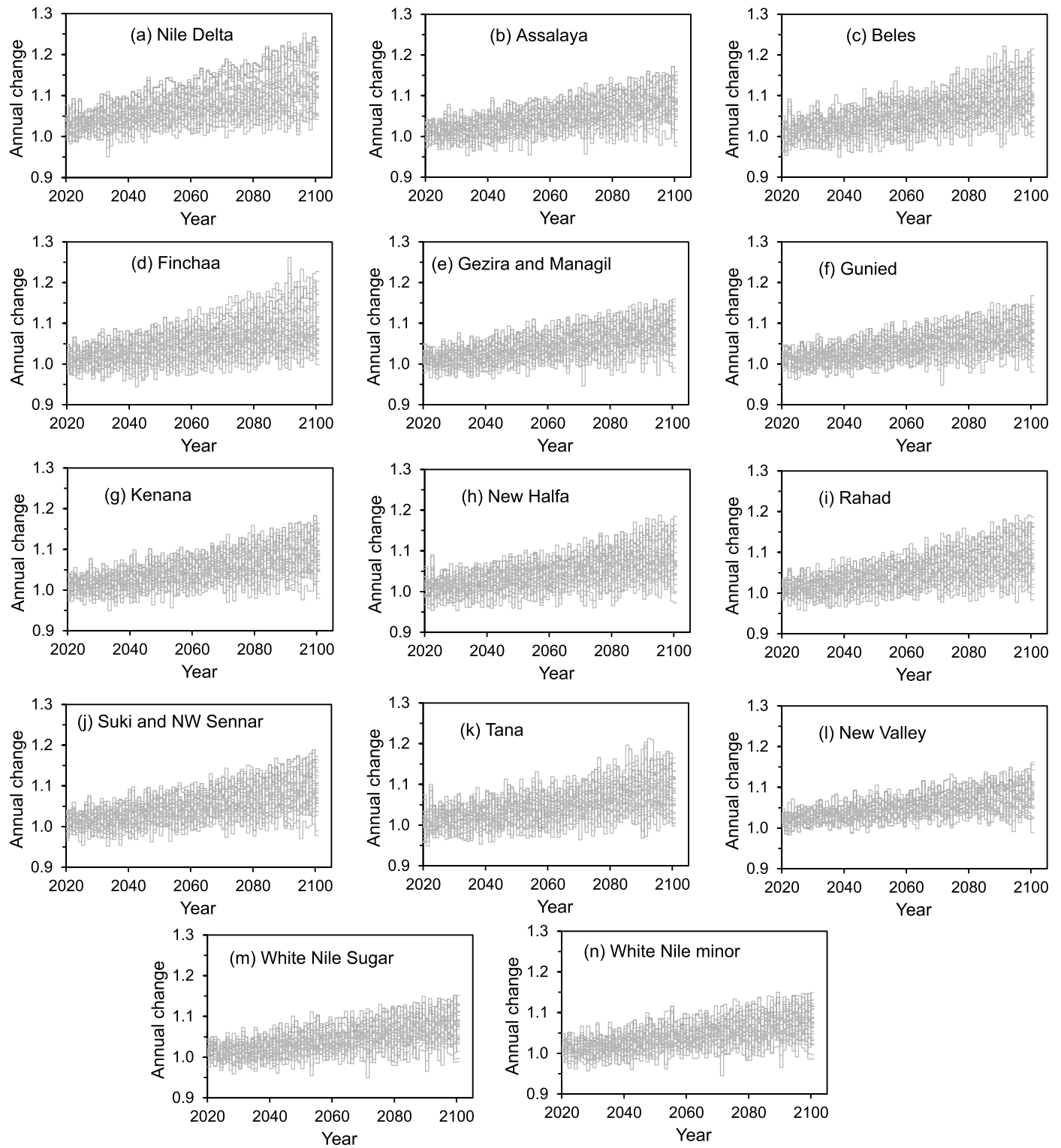
Extended Data Fig. 1 | Mean monthly naturalized streamflow calculated as a percentage of the mean annual naturalized streamflow. Mean monthly naturalized streamflow of the Nile Basin (a) and its major sub-basins (b–d).

Tekeze-Atbara is projected to witness the biggest change in the intra-annual naturalized streamflow variability under the most extreme scenarios, followed by the Blue Nile.

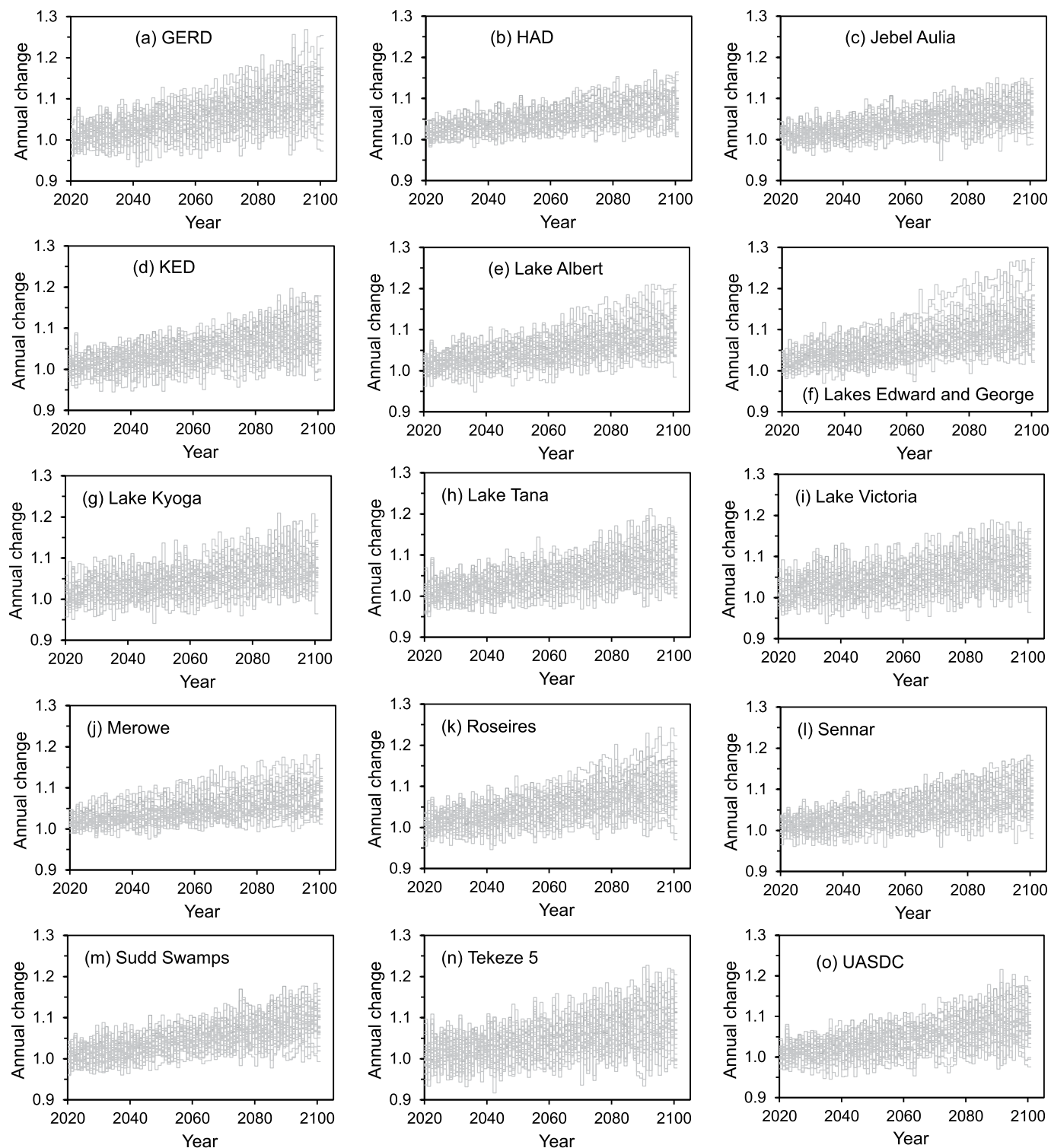


Extended Data Fig. 2 | Standardized streamflow index of the annual naturalized streamflow of the Nile Basin relative to the mean and standard deviation of 1981–2010. Standardized streamflow index for different climate change projections (a–ab). The index is calculated as follows: the annual

naturalized streamflow minus the mean annual naturalized streamflow in 1981–2010; this difference is divided by the standard deviation of the annual naturalized streamflow in 1981–2010.

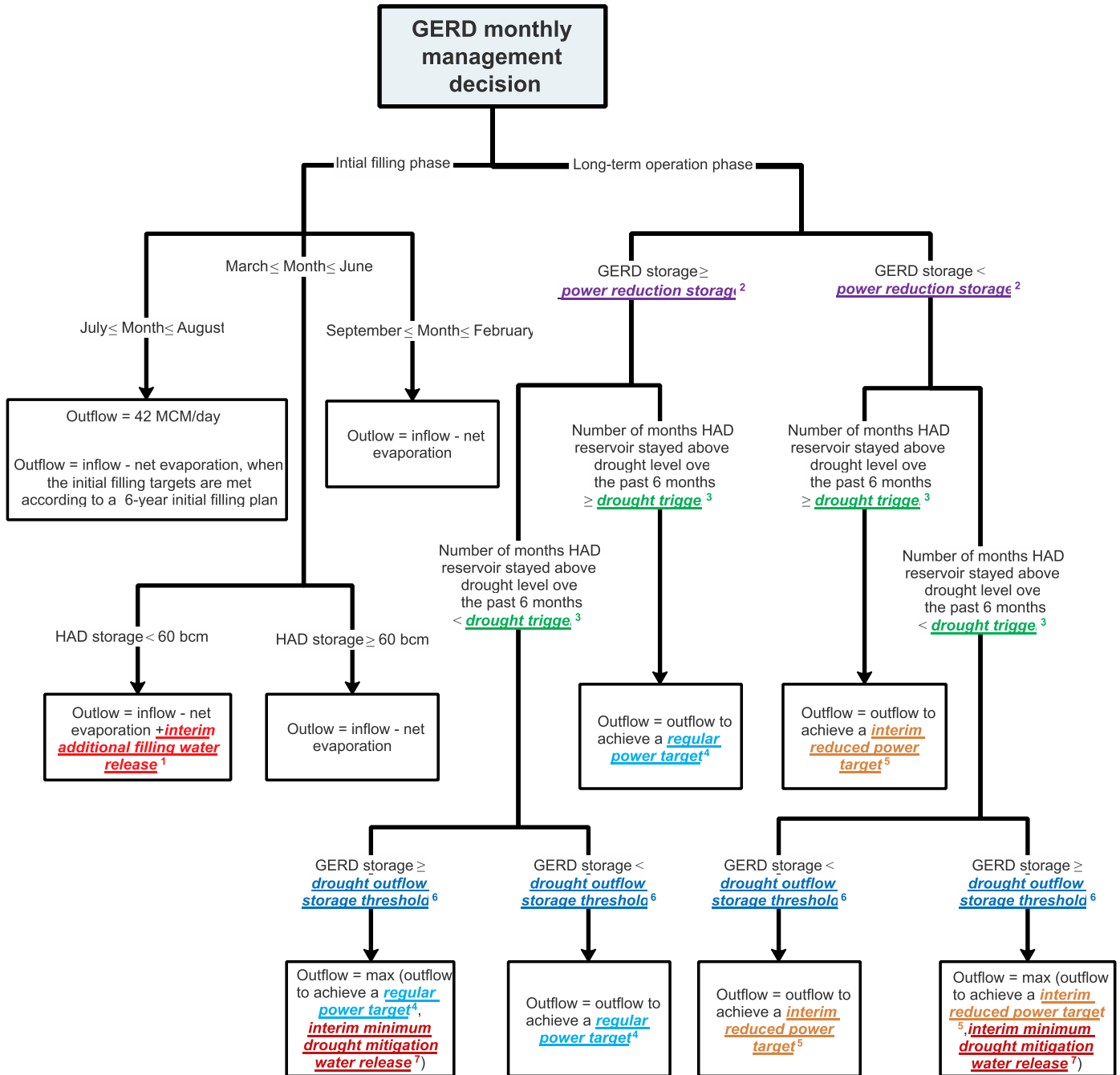


Extended Data Fig. 3 | Annual change in the mean potential evapotranspiration in large-scale irrigation schemes in the Nile Basin. The annual change values (a–n) are calculated with respect to the mean potential evapotranspiration in 1981–2010, such that change values higher than one indicate an increase in annual evapotranspiration.



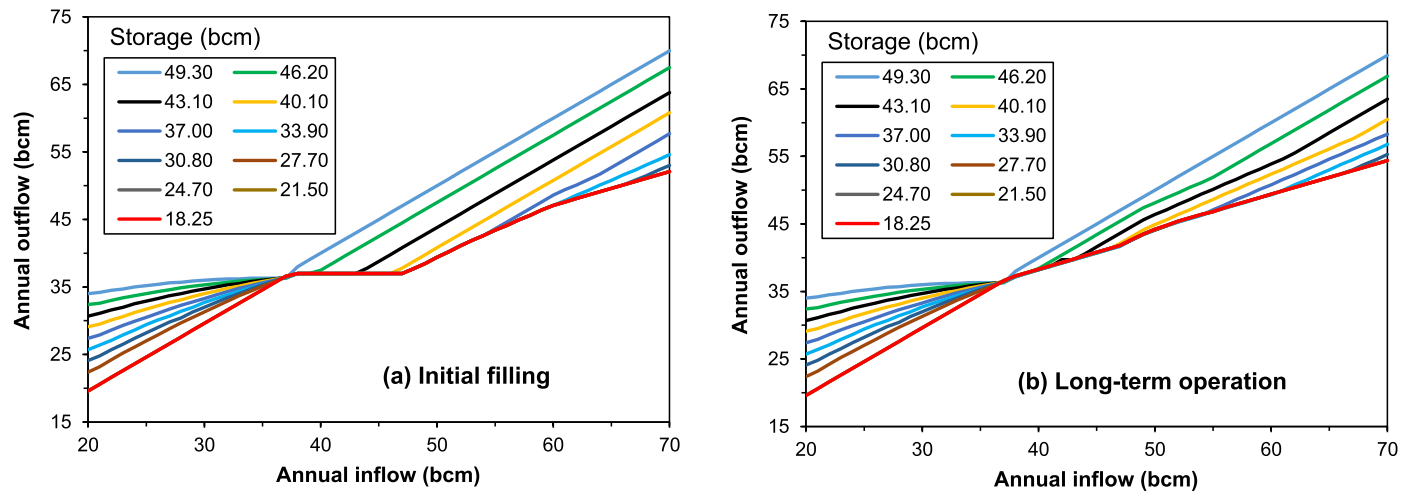
Extended Data Fig. 4 | Annual change in the mean potential evaporation rates from open water bodies in the Nile Basin. The annual change values (a–o) are calculated with respect to the mean potential evaporation rates in 1981–2010, such that change values higher than one indicate an increase in rates. Potential evaporation rates from open water bodies were calculated following

FAO56 recommendations using a multiplication factor applied to potential evapotranspiration. GERD stands for Grand Ethiopian Renaissance Dam, UASDC stands for Upper Atbara and Setit Dam Complex, KED stands for Khashm Elgirba Dam, D/S stands for downstream, and HAD stands for High Aswan Dam.



Extended Data Fig. 5 | Adaptive management policy of the Grand Ethiopian Renaissance Dam. The management policy shows the operation decisions for the Grand Ethiopian Renaissance Dam (GERD) in the initial filling and long-term operation phases. HAD stands for High Aswan Dam. Labels numbered from 1 to 7

are the decision variables in the multiobjective optimization problem. The labels numbered 3, 4, 5 and 7 are the decision variables adapted over time as climate change unfolds.



Extended Data Fig. 6 | Annual water release rules of the Grand Ethiopian Renaissance Dam under the Washington draft proposal. a, Initial filling. b, Long-term operation. The Washington draft proposal contains additional rules to mitigate the impacts of droughts, as described in Supplementary Section 2.

Reporting Summary

Nature Research wishes to improve the reproducibility of the work that we publish. This form provides structure for consistency and transparency in reporting. For further information on Nature Research policies, see our [Editorial Policies](#) and the [Editorial Policy Checklist](#).

Statistics

For all statistical analyses, confirm that the following items are present in the figure legend, table legend, main text, or Methods section.

n/a Confirmed

- The exact sample size (n) for each experimental group/condition, given as a discrete number and unit of measurement
- A statement on whether measurements were taken from distinct samples or whether the same sample was measured repeatedly
- The statistical test(s) used AND whether they are one- or two-sided
Only common tests should be described solely by name; describe more complex techniques in the Methods section.
- A description of all covariates tested
- A description of any assumptions or corrections, such as tests of normality and adjustment for multiple comparisons
- A full description of the statistical parameters including central tendency (e.g. means) or other basic estimates (e.g. regression coefficient) AND variation (e.g. standard deviation) or associated estimates of uncertainty (e.g. confidence intervals)
- For null hypothesis testing, the test statistic (e.g. F , t , r) with confidence intervals, effect sizes, degrees of freedom and P value noted
Give P values as exact values whenever suitable.
- For Bayesian analysis, information on the choice of priors and Markov chain Monte Carlo settings
- For hierarchical and complex designs, identification of the appropriate level for tests and full reporting of outcomes
- Estimates of effect sizes (e.g. Cohen's d , Pearson's r), indicating how they were calculated

Our web collection on [statistics for biologists](#) contains articles on many of the points above.

Software and code

Policy information about [availability of computer code](#)

Data collection No software was used

Data analysis The Python water resources simulation model (Pywr version 1.9.1) is open-source and freely available at: <https://github.com/pywr/pywr>, and building Pywr models can be facilitated by www.waterstrategy.org. The standard CGE model of the International Food Policy Research Institute is open-source and freely accessible through the following link: <https://www.ifpri.org/publication/standard-computable-general-equilibrium-cge-model-gams-0>. The Variable Infiltration Capacity (VIC version 5) model is freely accessible through the following link: <https://vic.readthedocs.io/en/master/>. The Routing Application for Parallel computation of Discharge (RAPID version 1.8.0) is freely accessible through the following link: <http://rapid-hub.org/index.html>. The Python Network Simulation framework (Pynsim version 0.1.5) is open-source and freely available in the following repository: <https://github.com/UMWRG/pynsim>. The multiobjective Non-dominated Sorting Genetic Algorithm (NSGA-III), the Multi-Objective Evolutionary Algorithm (MOEA) used in the multiobjective search, is open-source and freely available through Platypus version 1.0.4 in the following repository: <https://github.com/Project-Platypus/Platypus>. The Random Forest Regression Algorithm is open-source and freely available through Scikit-learn version 0.24.2 at: <https://github.com/scikit-learn/scikit-learn>.

For manuscripts utilizing custom algorithms or software that are central to the research but not yet described in published literature, software must be made available to editors and reviewers. We strongly encourage code deposition in a community repository (e.g. GitHub). See the Nature Research [guidelines for submitting code & software](#) for further information.

Data

Policy information about [availability of data](#)

All manuscripts must include a [data availability statement](#). This statement should provide the following information, where applicable:

- Accession codes, unique identifiers, or web links for publicly available datasets
- A list of figures that have associated raw data
- A description of any restrictions on data availability

The economy-related input data supporting this study's findings are available at Zenodo: <http://doi.org/10.5281/zenodo.5914757>. The Nile River system model and its data are not publicly available due to state restrictions and contain information that could compromise research participant privacy/consent. The Nile model data can be made available upon presentation of necessary permissions from the relevant authorities that own the data. The CMIP6 climate projections data can be accessed from: <https://esgf-node.llnl.gov/search/cmip6/>. The baseline population, labor, urbanization, and economic growth data of Ethiopia, Sudan, and Egypt associated with the SSPs can be accessed from the International Institute for Applied System Analysis (IIASA) database: <https://tntcat.iiasa.ac.at/SspDb/dsd?Action=htmlpage&page=10>. The sectoral productivity projections of Ethiopia, Sudan, and Egypt were produced based on data from the Centre d'Études Prospectives et d'Informations Internationales (CEPII): http://www.cepii.fr/cepii/en/bdd_modele/bdd.asp. The Multi-Source Weighted-Ensemble Precipitation (MSWEP) data are available from: <http://www.gloh2o.org/mswep/>. The Princeton Global Forcing (PGF) data are available from: <https://rda.ucar.edu/datasets/ds314.0/>. The river network data used with the Routing Application for Parallel computation of Discharge (RAPID) are freely accessible from: <https://www.hydrosheds.org/>. The World Bank data referred to in the manuscript is freely accessible from: <https://data.worldbank.org/>.

Field-specific reporting

Please select the one below that is the best fit for your research. If you are not sure, read the appropriate sections before making your selection.

- Life sciences Behavioural & social sciences Ecological, evolutionary & environmental sciences

For a reference copy of the document with all sections, see [nature.com/documents/nr-reporting-summary-flat.pdf](https://www.nature.com/documents/nr-reporting-summary-flat.pdf)

Ecological, evolutionary & environmental sciences study design

All studies must disclose on these points even when the disclosure is negative.

Study description	This study introduces the first planning framework for adaptive management of river infrastructure systems to consider both the socio-economic and hydrological uncertainties of climate change and policy. The framework uses climate and socio-economic data from the Coupled Model Intercomparison Project 6 (CMIP6) to drive integrated hydrological, economy-wide, and river system simulators of the Nile Basin. Our adaptive planning framework uses artificial intelligence-based algorithms to design efficient adaptive plans for climate change. We use the framework to design a cooperative adaptive management policy for the Grand Ethiopian Renaissance Dam (GERD) that considers the socio-economic and river system interests of Ethiopia, Sudan, and Egypt.
Research sample	The targeted region of the study is the Nile Basin. The Nile River Basin, located in northeastern Africa, faces the threat of climate change alongside physical and economic water scarcities, rapidly rising pressures on water resources due to population and economic growth, and a politically complex transboundary water management system
Sampling strategy	Twenty climate projections were selected from CMIP6 Tier-1 based on uniform sampling to cover the full range of available SSPs, radiative forcing, and the joint distribution of EOC change in precipitation and temperature over the Nile Basin. Processing and bias correction of the GCM simulations was driven by the requirement for transient (2017-2100) 3-hourly forcing data across seven climate variables that govern the surface mass and energy balances in the hydrological model. We developed nine additional projections based on 9 of the 20 initial projections by removing the overall wetting tendency in the CMIP6 ensemble for this region.
Data collection	The CMIP6 climate projections data were obtained from: https://esgf-node.llnl.gov/search/cmip6/ . The baseline population, labor, urbanization, and economic growth data of Ethiopia, Sudan, and Egypt associated with the SSPs were obtained from the International Institute for Applied System Analysis (IIASA) database: https://tntcat.iiasa.ac.at/SspDb/dsd?Action=htmlpage&page=10 . The sectoral productivity projections of Ethiopia, Sudan, and Egypt were produced based on data from the Centre d'Études Prospectives et d'Informations Internationales (CEPII): http://www.cepii.fr/cepii/en/bdd_modele/bdd.asp . The Multi-Source Weighted-Ensemble Precipitation (MSWEP) data were obtained from: http://www.gloh2o.org/mswep/ . The Princeton Global Forcing (PGF) data were obtained from from: http://hydrology.princeton.edu/data.pgf.php .
Timing and spatial scale	The overall timeframe of the study is 1979-2100, including climate data downscaling and bias-correction (1979-2100), hydrological model development and simulation (1979-2100), economy simulation (2011-2045), and river system infrastructure simulation (1995-2045). The spatial domain of the study is the Nile Basin.
Data exclusions	No data were excluded from the analysis.
Reproducibility	The study experiments were designed based on numerical simulations. To ensure that the study experiments are reliable and reproducible, we calibrated and validated the simulation models at multiple sites in the Nile Basin over multi-year periods.
Randomization	The Nile river system simulator was calibrated over the period 1995-2004 and validated over the period 2005-2010 at ten locations over using historical river flow observations and reservoir and lake water levels. This calibration period was chosen based on the availability of common and continuous historical observed data for the ten selected locations.

Blinding

Binding is not relevant to the data because our data are acquired and processed systematically with established computational pipelines.

Did the study involve field work? Yes No

Reporting for specific materials, systems and methods

We require information from authors about some types of materials, experimental systems and methods used in many studies. Here, indicate whether each material, system or method listed is relevant to your study. If you are not sure if a list item applies to your research, read the appropriate section before selecting a response.

Materials & experimental systems

- | n/a | Involvement in the study |
|-------------------------------------|--|
| <input checked="" type="checkbox"/> | <input type="checkbox"/> Antibodies |
| <input checked="" type="checkbox"/> | <input type="checkbox"/> Eukaryotic cell lines |
| <input checked="" type="checkbox"/> | <input type="checkbox"/> Palaeontology and archaeology |
| <input checked="" type="checkbox"/> | <input type="checkbox"/> Animals and other organisms |
| <input checked="" type="checkbox"/> | <input type="checkbox"/> Human research participants |
| <input checked="" type="checkbox"/> | <input type="checkbox"/> Clinical data |
| <input checked="" type="checkbox"/> | <input type="checkbox"/> Dual use research of concern |

Methods

- | n/a | Involvement in the study |
|-------------------------------------|---|
| <input checked="" type="checkbox"/> | <input type="checkbox"/> ChIP-seq |
| <input checked="" type="checkbox"/> | <input type="checkbox"/> Flow cytometry |
| <input checked="" type="checkbox"/> | <input type="checkbox"/> MRI-based neuroimaging |